

Induction of Supramolecular Chirality

M.Sc. Thesis

By

ANTARA REJA



DISCIPLINE OF CHEMISTRY
INDIAN INSTITUTE OF TECHNOLOGY INDORE
JULY, 2017

Induction of Supramolecular Chirality

A THESIS

*Submitted in partial fulfillment of the
requirements for the award of the degree
of*
Master of Science

by
ANTARA REJA



**DISCIPLINE OF CHEMISTRY
INDIAN INSTITUTE OF TECHNOLOGY
INDORE
JULY, 2017**



INDIAN INSTITUTE OF TECHNOLOGY, INDORE

CANDIDATE'S DECLARATION

I hereby certify that the work which is being presented in the thesis entitled **Induction of Supramolecular Chirality** in the partial fulfillment of the requirements for the award of the degree of **MASTER OF SCIENCE** and submitted in the **DISCIPLINE OF CHEMISTRY, Indian Institute of Technology Indore**, is an authentic record of my own work carried out during the time period from JULY 2016 to JULY 2017 under the supervision of Dr. Apurba Kumar Das, Discipline of chemistry, Indian Institute of Technology, Indore

The matter presented in this thesis has not been submitted by me for the award of any other degree of this or any other institute.

ANTARA REJA

This is to certify that the above statement made by the candidate is correct to the best of my/our knowledge.

Dr. APURBA K.DAS

ANTARA REJA has successfully given her M.Sc. Oral Examination held on

Signature of Supervisor of MSc thesis

Date:

Convener, DPGC

Date:

Signature of PSPC Member

Date:

Signature of PSPC Member

Date:

ACKNOWLEDGEMENTS

Foremost, I would like to express my sincere gratitude to my advisor Dr. Apurba K. Das for the continuous support of my M.Sc. study and my research, for his patience, motivation, enthusiasm, and immense knowledge. His guidance helped me all the time of research and writing of this thesis. I could not have imagined having a better advisor and mentor for my M.Sc. study.

I would like to thank my thesis committee members, my senior group members and also to my class mates for their valuable comments and suggestions for the improvement of the thesis.

I extend my profound thanks to SIC, IIT Indore, for providing instrument facilities.

Last but not the least, I would like to thank my parents for their unconditional love and support in every way and guiding me spiritually throughout my life, above all the others, for always going above and beyond in terms of their love and support.

Antara Reja

M.Sc. II year

Discipline of Chemistry

IIT INDORE

Dedicated to my

Father

for his immense selfless love towards me

Abstract

Base catalyzed methyl ester hydrolysis of discotic C_3 symmetric benzene-1,3,5-tricarboxamides coupled with (L) and (D) phenylalanine were found to self-assemble into supramolecular gels with helical morphological features. The handedness of macroscopic chirality was tuned by the chiral amino acids attached with the periphery of benzene-tri-carboxamides which were revealed by circular dichroism, scanning electron microscopy and transmission electron microscopic studies. Thixotropic and self-healing properties of the supramolecular gels were also assessed.

TABLE OF CONTENTS

LIST OF FIGURES	viii-ix
LIST OF TABLES	x
LIST OF SCHEMES	x
NOMENCLATURE	xi
ACRONYMS	xii

Chapter 1: Introduction and reaction scheme	1-6
--	------------

1.1 Introduction	1-3
------------------	-----

1.2 Scheme	4-6
------------	-----

Chapter 2: Experimental sections	7-13
---	-------------

2.1 Materials:	7
----------------	---

2.2 Synthesis of compounds:	7-9
-----------------------------	-----

2.2.1 Synthesis of compound 1	7-8
-------------------------------	-----

2.2.2 Synthesis of compound 2	8-9
-------------------------------	-----

2.2.3 Preparation of (L)-gel	9
------------------------------	---

2.2.4 Preparation of (D)-gel	9
------------------------------	---

2.3 General methods:	9
----------------------	---

2.4 High performance liquid chromatography (HPLC) analysis:	10
2.5 FT-IR study:	10-11
2.6 Circular dichroism (CD) study:	11
2.7 Morphological study:	11
2.8 Wide angle X-ray diffraction study:	11-12
2.9 UV-Visible spectroscopy:	12
2.10 Fluorescence spectroscopy:	12
2.11 Rheological measurements and self-healing property:	12-13

Chapter 3: Results and discussion

3.1 Synthesis of the compounds:	13
3.2 HPLC analysis and mass spectrometry:	14-15
3.3 FT-IR study of gelators and gels:	15-18
3.4 Circular dichroism study of gels:	19
3.5 Morphological study of gels:	20
3.6 Wide angle XRD study of gelators and dried gels:	21-22

3.7 UV-Vis spectroscopy of gelators and gels:	23-24
3.8 Fluorescence spectroscopy:	24-25
3.9 Rheological study of the gels:	25-29
3.10 Hydrolysis of compound 1 and compound 2 by using different bases:	29-30
Chapter 4: Conclusion	31
APPENDIX-A:	32-36
REFERENCES:	37-47

LIST OF FIGURES

Figure No.	Description	Page No.
Fig. 1:	HPLC analysis and mass spectra of compound 1 and (L)-gel	14
Fig. 2:	HPLC analysis and mass spectrometry of compound 2 and (D)-gel	15
Fig. 3:	FT-IR spectrum of compound 1	16
Fig. 4:	FT-IR spectrum of (L)-gel	17
Fig. 5:	FT-IR spectrum of compound 2	17
Fig. 6:	FT-IR spectrum of (D)-gel	18
Fig. 7:	CD spectrum of (L) and (D)-gel	19
Fig. 8:	SEM and TEM images of (L) and (D)-gels	20
Fig. 9:	Wide angle XRD of compound 1 and it's xerogel	21
Fig. 10:	Wide angle XRD of compound 2 and it's xerogel	22
Fig. 11:	Proposed self-assembly mechanism elucidated by PXR	22
Fig. 12:	UV-Vis spectra of compound 1 and it's gel	23
Fig. 13:	UV-Vis spectra of compound 1 and it's gel	24
Fig. 14:	Emission and excitation spectra (L)-gel	24

Fig. 15: Emission and excitation spectra (D)-gel	25
Fig. 16: Photographic images of (L) and (D)-gels under UV-visible light	25
Fig. 17: Dynamic frequency sweep of self-assembled (L)-gel at constant strain 0.01%	27
Fig. 18: Dynamic frequency sweep of self-assembled (D)-gel at constant strain 0.01%	28
Fig. 19: Hysteresis loop test of self-assembled (L)-gel	28
Fig. 20: Hysteresis loop test of self-assembled (D)-gel	29
Fig. 21: Self-healing behavior of (L) gel	29
Fig. 22: Hydrolysis of compound 1 and 2 by using LiOH	30
Fig. 23: Hydrolysis of compound 1 and 2 by using NaOH	30
Fig. 24: Hydrolysis of compound 1 and 2 by using KOH	30
Fig. 25: 400 MHz ¹H NMR spectrum of compound 1 in CDCl₃	32
Fig. 26: 100 MHz ¹³C NMR spectrum of compound 1 in CDCl₃	33
Fig. 27: 400 MHz ¹H NMR spectrum of compound 2 in CDCl₃	33
Fig. 28: 100MHz ¹³C NMR spectrum of compound 2 In CDCl₃	34
Fig. 29: ESI-MS spectrum of compound 1	34

Fig. 30:ESI-MS spectrum of (L)-gel	35
Fig. 31:ESI-MS spectrum of compound 2	35
Fig. 32:ESI-MS spectrum of (D)-gel	36

LIST OF TABLES

Table No.	Description	Page No.
Table 1:	FT-IR stretching frequencies of the compounds	18
Table 2:	Hydrolysis of the compound 1 and 2 by using different bases	29

LIST OF SCHEMES

Scheme No.	Description	Page No.
Scheme 1:	Self-assembly of monomeric units into helical superstructure	4
Scheme 2:	Chemical structures and synthetic scheme of compound 1 and it's gel	5
Scheme 3:	Chemical structures and synthetic scheme of compound 2 and it's gel	6

NOMENCLATURE

θ	Angle
A°	Angstrom
cm	Centimeter
nm	Nanometer
π	pi
λ	Wavelength

ACRONYMS

Abbreviations used for compounds, substituents, reagents, etc. are largely in accordance with the recommendations of the IUPAC. Additional abbreviations used in this thesis are listed below

CDCl ₃	Chloroform d
DMSO d ₆	Dimethyl Sulfoxide d ₆
DMF	Dimethyl formamide
d	Doublet
EtOH	Ethanol
EtOAc	Ethyl Acetate
ESI-MS	Electron Ionization Mass Spectrometry
HCL	Hydrochloric Acid
LiOH	Lithium Hydroxide
MeOH	Methanol
NMR	Nuclear Magnetic Resonance
s	Singlet
THF	Tetrahydrofuran
TLC	Thin Layer Chromatography
t	triplet
UV-Vis	UV- Visible

Chapter 1: Introduction and Reaction scheme

1.1 Introduction:

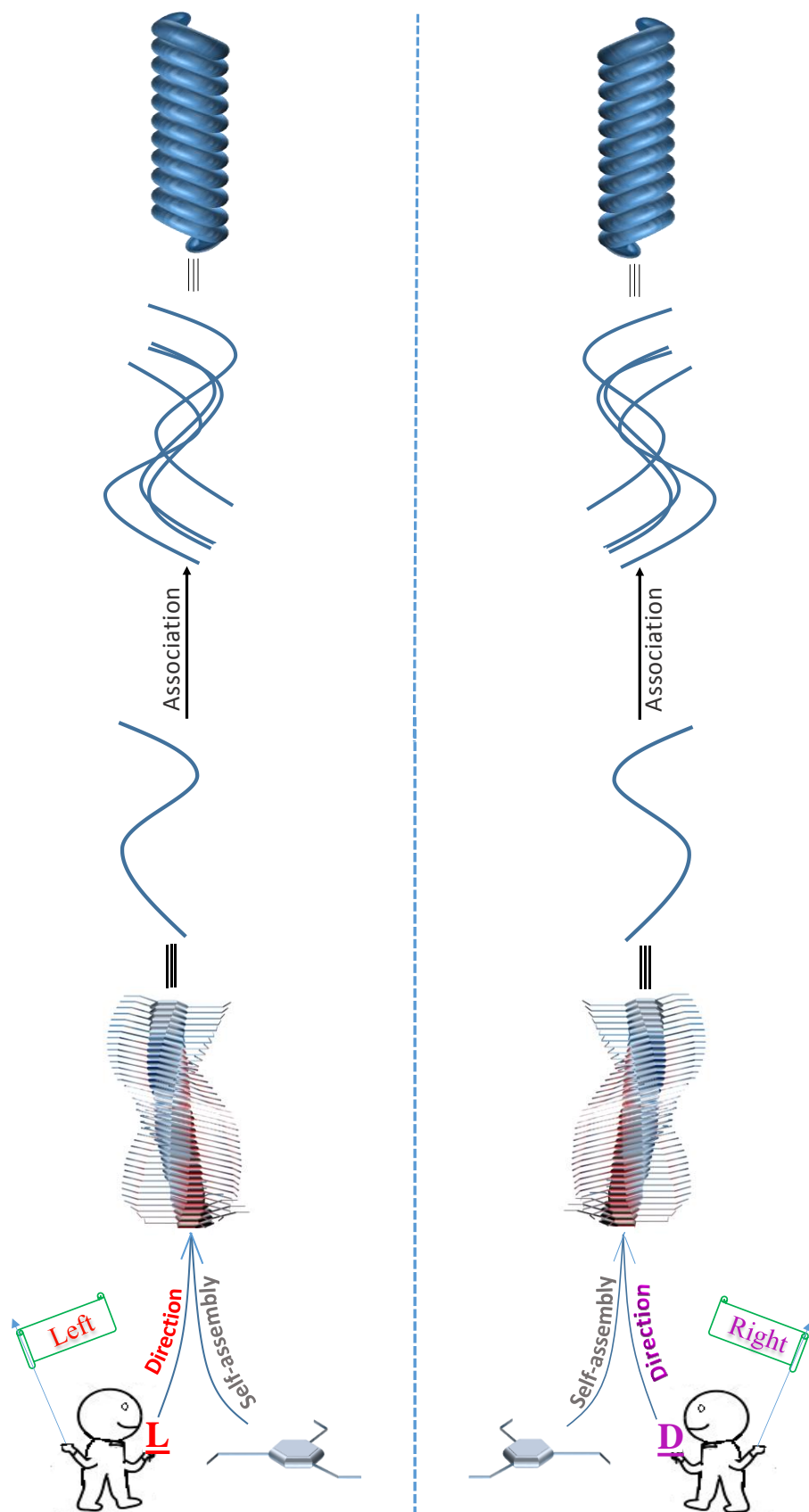
Supramolecular chirality is a unique evolution in nature that reveals the chirality at supramolecular level. Supramolecular chirality arises due to the involvement of non-covalent interactions¹⁻² like hydrogen bonding, van der Waals interactions, π - π stacking and hydrophobic interactions³⁻⁵ as well as the influence of chiral building blocks in the system. These forces perceive over a wide region that start from molecular level and extend up to supramolecular level.⁶ Supramolecular chirality has attracted more attention in the research field due to its various applications in the areas of catalysis,⁷⁻⁸ non-linear optics,⁹ polymer and materials science,¹⁰⁻¹² molecular recognition,¹³⁻¹⁴ molecular device,¹⁵⁻¹⁷ and absolute configuration determination.¹⁸⁻²⁰ To induce the chirality within the supramolecular system, it is not necessary that the building block should be chiral. Sometimes achiral constituents can also provoke supramolecular chirality.²¹⁻²⁴ However, chiral micro-environments are fabricated with the use of chiral building blocks which offer an additional factor to induce chirality within the supramolecular system.²⁵⁻³¹ Supramolecular gel, a self-binding soft matter,³² is constructed based on the arrangement of low molecular weight gelator units (LMWGs) in a hierarchical manner through non-covalent interactions, which can form different morphological structures such as nanorods,³³⁻³⁵ nanoribbons, nanotubes, nanotwist³⁶⁻³⁸ and microtubes.³⁹⁻⁴¹ The formation of different morphological structures depends on the structure of the monomer,⁴² functional groups present in monomer, assembly rate,⁴³ change in pH,⁴⁴⁻⁴⁵ ultrasound,⁴⁶⁻⁴⁸ redox potential⁴⁹ and solvent-solute interactions.⁵⁰⁻⁵⁴ Nanohelix is one of the most fascinating nanostructures that is formed by the self-assembly of the building blocks due to their various applications in chemistry,⁵⁵⁻⁵⁸ biology⁵⁹⁻⁶⁰ and materials sciences.⁶¹⁻⁶⁴ After a detailed survey of the previous studies, it was found that (L)- amino acid based derivatives

favour to form right-handed helical structure and (D)-amino acid based derivatives appropriate the opposite one. However, there are few reports where (L)-amino acid derivatives produced left-handed helical structure.⁶⁵ So, chirality of the monomeric unit is not a convenient parameter to fabricate the chirality at supramolecular level. Supramolecular chirality also depends on other parameters. Chirality of supramolecular gel systems depends on the arrangement, chirality of the gelators and solvent-solute interactions.⁶⁶⁻⁶⁹ Here, so called memory effect⁷⁰ is responsible for transferring the proper chiral information from one gelator unit to another gelator unit which helps to induce the chirality within this supramolecular system.⁷¹⁻⁷² As a result, chirality is directly transferred from the molecular building block units to supramolecular structures which help to tune the chirality within the whole supramolecular system.⁷³ The control of chirality in synthetic self-assembled systems is very important for the applications in molecular recognition, mimicking of catalytic activity of enzymes and in the field of asymmetric catalysis.⁷⁴ Meijer *et al* have explained co-operative self-assembly between C₃ symmetrical chiral molecule and its achiral analog according to the ‘sergeants and soldiers’ principle. The chiral sergent strongly amplifies the handedness of the mixed stacks.⁷⁵ Liu *et al* demonstrated that C₃ symmetrical benzene-1,3,5-tricarboxamide substituted with achiral ethyl cinnamate self-assembled to form mixed right handed and left handed twisted morphological structures. However, introduction of chiral building blocks tuned the handedness and macroscopic chirality of the self-assembled gels.²⁴ Zhao *et al* reported that achiral bipyridines formed right handed helical nanostructures in a cooperative self-assembly with (L)-phenylalanine derivative through hydrogen bonding interactions formed between the pyridyl and carboxylic acid groups.⁷⁶

In this work, the role of chiral configuration of two enantiomeric amino acids attached with benzene-1,3,5-tricarboxamides to tune the spatial arrangement of the building block units from the

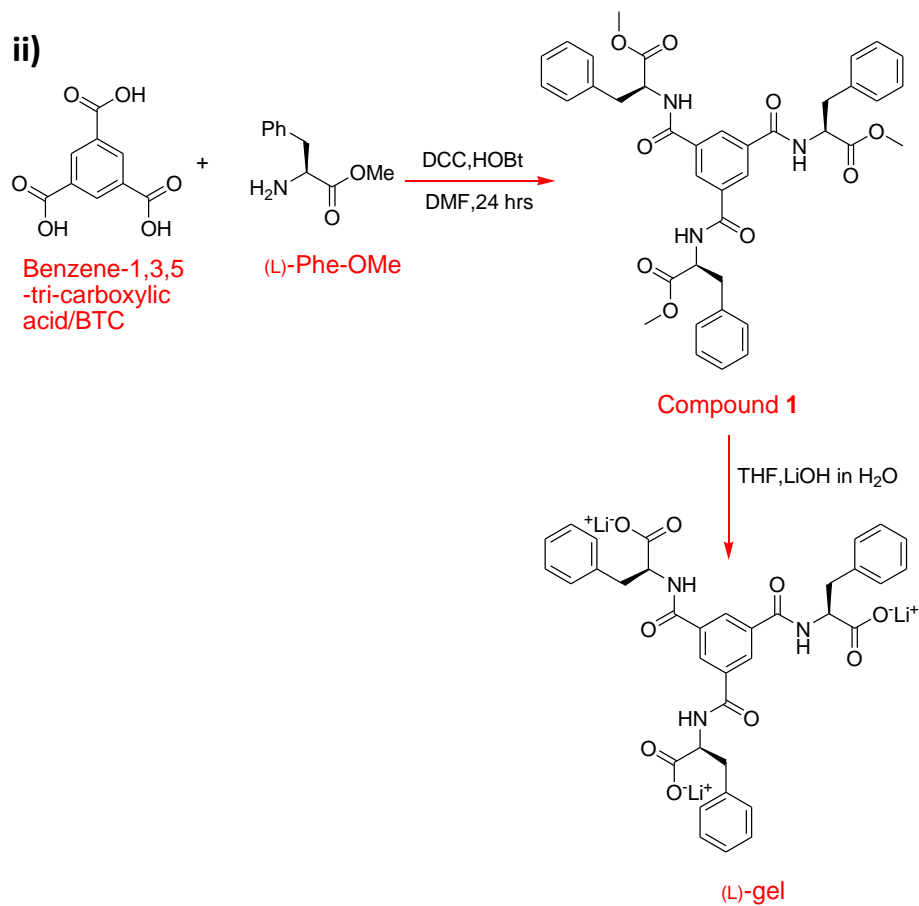
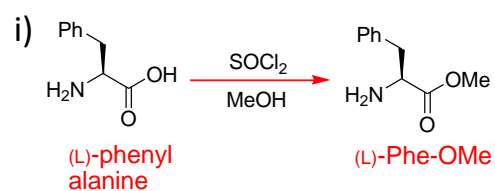
molecular level to the supramolecular level was one of our objectives. Herein, acid-amine coupling reaction was carried out between benzene-1,3,5-tricarboxylic acid (BTC) and methyl esters of (L)-phenylalanine (L-Phe-OMe) and (D)-phenylalanine (D-Phe-OMe). Both enantiomeric triamides formed gels in reaction medium during hydrolysis by 1M aqueous LiOH solution in THF solution. Circular dichroism spectra, scanning electron microscopy, transmission electron microscopy images confirmed that two enantiomers formed opposite helical fibrillar structures.

Here, the chirality,⁷⁷⁻⁸² the arrangement of the building block units and increasing structural complexity during the origin of the supramolecular structures from the monomeric units⁸³ act as the executive parameter to determine the handedness of the structure from helix to fiber.⁸⁴

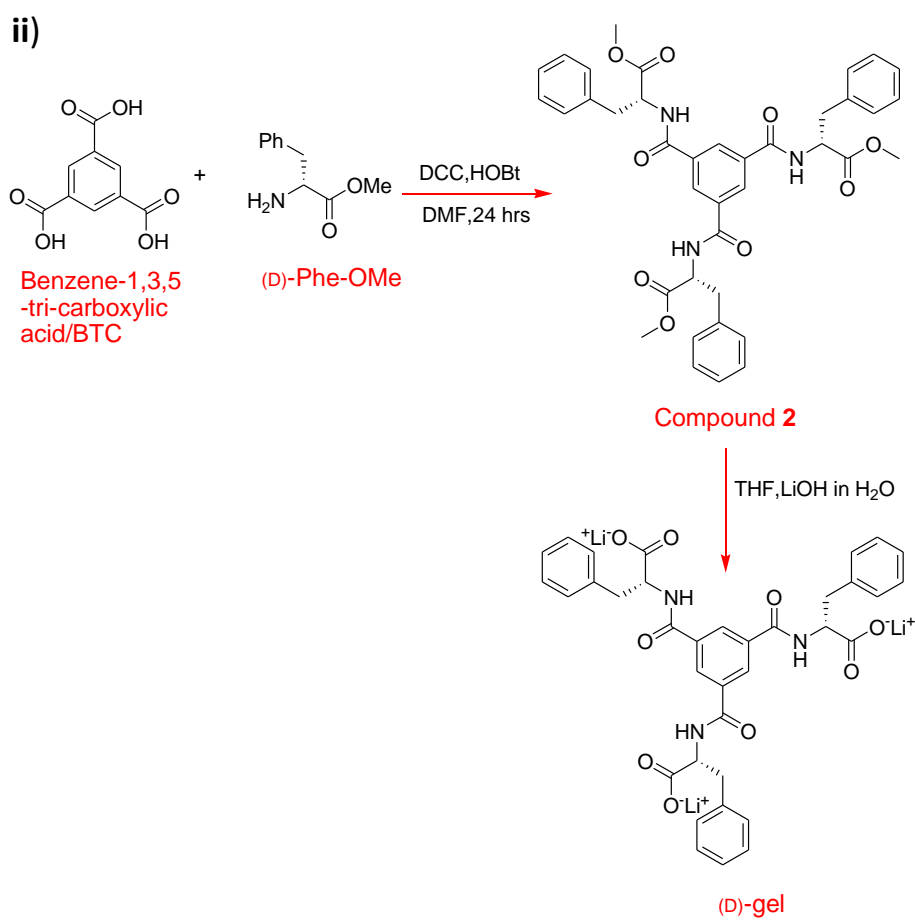
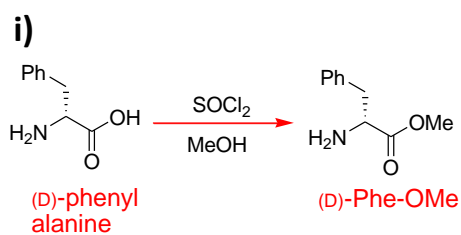


Scheme 1: Self-assembly of (L) monomeric units into left handed and (D) monomeric units into right handed helical superstructures

1.2 Reaction Scheme:



Scheme 2: Chemical structures and synthetic scheme of compound 1 and its corresponding (L)-gel



Scheme 3: Chemical structures and synthetic scheme of compound 2 and its corresponding (D)-gel

Chapter 2: Experimental sections

2.1 Materials:

All of the amino acids, benzene-1,3,5-tricarboxylic acid were purchased from Sigma-Aldrich, U.S.A. N,N'-dicyclohexylcarbodiimide and 1-hydroxybenzotriazole were acquired from Sisco Research Laboratories Pvt. Ltd. (SRL), Mumbai, India

2.2 Synthesis of compounds:

Synthesis of Benzene Tricarboxamide (BTCA). C-terminal end of both (D) and (L) phenylalanine was protected by methyl ester. C-terminus protected amino acid was coupled with benzene tricarboxylic acid in dimethyl formamide followed by addition of N,N'-dicyclohexylcarbodiimide and 1-hydroxybenzotriazole (DCC-HOBt). Final compounds were purified by flash chromatography and fully characterized by ^1H NMR, ^{13}C NMR, ESI-MS and FT-IR studies.

2.2.1 Synthesis of *BTC-(L-Phe-OMe)*₃ / Compound 1: 0.5 gm (2.38 mmol) of benzene-1,3,5-tricarboxylic acid in 5 mL DMF was cooled in an ice bath. (L)-Phe-OMe was isolated from 2.3 gm (10.71 mmol) of the corresponding methyl ester hydrochloride by neutralization and subsequent extraction with ethyl acetate, and the ethyl acetate extract was concentrated to 4 mL. It was then added to the reaction mixture followed immediately by 1.77 gm (8.56 mmol) of DCC, 0.96 gm (7.14 mmol) of HOBt. The reaction mixture was stirred overnight. The progress of the reaction was monitored by thin layer chromatography (TLC). Then ethyl acetate (50 mL) was added to the reaction mixture

and DCU was filtered off. The organic layer was washed with 1 M HCl (3×50 mL), brine (2×50 mL), 1 M sodium carbonate (3×50 mL) and brine (2×50 mL) and dried over anhydrous sodium sulfate and evaporated under vacuum to yield (**1**) as a white solid. Purification was done by flash chromatography using hexane-ethyl acetate (1:1) as eluent.

Yield: 0.4gm (0.58 mmol, 80%). FT-IR (KBr): $\tilde{\nu}$ 3225.12 (broad), 1748.27 (s), 1641.34 (s), 1560.65 (s), 1219.29 (s) cm^{-1} . ^1H NMR (400 MHz, CDCl_3 , δ): 8.06 (s, 3H, Ar-Hs of BTC), 7.32-7.12 (m, 18H, 15 Ar-Hs of Phe(1), Phe(2), Phe(3) and 3 NHs of Phe(1), Phe(2), Phe(3)), 4.99-4.96 (q, $J = 12.64$ Hz, 3H, C^αHs of Phe(1), Phe(2) and Phe (3)), 3.68(s, 9H, -COOMe). 3.21-3.10 (dd, 6H, C^βHs of Phe(1), Phe(2) and Phe (3)) ppm. ^{13}C NMR (100 MHz, CDCl_3 , δ): 172.58, 165.29, 136.10, 134.39, 129.10, 54.21, 52.54, 37.76 ppm. MS (ESI) m/z ($\text{M}+\text{Na}$) $^+$ Calcd for $\text{C}_{39}\text{H}_{39}\text{O}_9\text{H}_3$: 716.2579; found: 716.2592.

2.2.2. Synthesis of BTC-(D-Phe-OMe)₃ / Compound 2: 0.5 gm (2.38 mmol) of benzene-1,3,5-tricarboxylic acid in 5 mL of DMF was cooled in an ice bath. (D)-Phe-OMe was isolated from 2.30 gm (10.71 mmol) of the corresponding methyl ester hydrochloride by neutralization and subsequent extraction with ethyl acetate and the ethyl acetate extract was concentrated to 4.2 mL. It was then added to the reaction mixture followed immediately by 1.77 gm (8.56 mmol) of DCC, 0.96 gm (7.14 mmol) of HOBt. The reaction mixture was stirred overnight. The progress of the reaction was monitored by thin layer chromatography (TLC). Then, ethyl acetate (50 mL) was added to the reaction mixture and DCU was filtered off. The organic layer was washed with 1 M HCl (3×50 mL), brine (2×50 mL), 1 M sodium carbonate (3×50 mL) and dried over anhydrous sodium sulfate and evaporated under vacuum to yield (**2**) as a white solid. Purification was done by flash chromatography using hexane-ethyl acetate (1:1) as eluent.

Yield: 0.42 gm (0.60 mmol, 84%). FT-IR (KBr): $\tilde{\nu} = 3225.12$ (broad), 1748.24 (s), 1641.34 (s), 1560.65 (s), 1219.29 (s) cm^{-1} . ^1H NMR (400

MHz, CDCl₃, δ): 8.11 (s, 3H, Ar-Hs of BTC), 7.23-7.08 (m, 18H, 15 Ar-Hs of Phe(1), Phe(2), Phe(3) and 3 NHs of Phe(1), Phe(2), Phe(3)), 5.01-4.98 (q, $J = 12.64$ Hz, 3H, C^αHs of Phe(1), Phe(2) and Phe(3)), 3.69 (s, 9H, -COOMe group), 3.23-3.10 (dd., C^βHs of Phe(1), Phe(2) and Phe(3)) ppm. ¹³C NMR (100 MHz, CDCl₃, δ): 172.64, 165.33, 136.16, 134.48, 129.22, 128.69, 54.27, 52.62, 37.85 ppm. MS (ESI) m/z (M+Na)⁺ Calcd for C₃₉H₃₉O₉H₃: 716.2579; found: 716.2588.

Preparation of Gel.

2.2.3 Preparation of (L)-gel: 60 mg (17.31 mmol) of BTC-(L-Phe-OMe)₃ **1** was dissolved in 5 mL tetrahydrofuran. Then 300 μL of 1(N) LiOH was added to the solution dropwise. The solution was allowed to stir for 4 h and (L)-gel was formed.

FT-IR (KBr): $\tilde{\nu}$ 3357 (broad), 3063 (w), 1630 (s), 1406 (s), 1291 (s), 1100 (s). MS (ESI) m/z (M-H)⁻ Calcd for C₃₆H₃₃O₉N₃: 650.2133; found: 650.2145.

2.2.4 Preparation of (D)-gel: Similarly, (D)-gel was also prepared.

FT-IR (KBr): $\tilde{\nu}$ 3338 (broad), 3057 (w), 1635 (s), 1410 (s), 1290 (s), 1102 (s). MS (ESI) m/z (M-H)⁻ Calcd for C₃₆H₃₃O₉N₃: 650.2133; found: 650.2123.

2.3 General Methods:

All NMR characterizations were carried out on a Bruker AV 400 MHz spectrometer at 300 K. Compound concentrations were in the range 5–10 mmol L⁻¹ in CDCl₃. Mass spectra were recorded on a Bruker micrOTOF-Q II by positive mode and negative mode electrospray ionizations

2.4. High performance liquid chromatography (HPLC)

analysis:

A Dionex HPLC-Ultimate 3000 (High Performance Liquid Chromatography) pump was used to analyze compounds **1** and **2** and base catalyzed hydrolyzed products. 20 μL of sample was injected onto a Dionex Acclaim® 120 C 18 column of 250 mm length with an internal diameter 4.6 mm and 5 μm fused silica particles at a flow rate of 1 mL min^{-1} (linear gradient of 40% v/v acetonitrile in water for 35 min, gradually rising to 100% (v/v) acetonitrile in water at 35 min). This concentration was kept constant until 40 min. The sample preparation was involved mixing of 100 μL of gel/solution with acetonitrile water (900 μL , 50: 50 mixture) containing 0.1% trifluoroacetic acid. The samples were then filtered through a 0.45 μm syringe filter (Whatman, 150 units, 13 mm diameter, 2.7 mm pore size) prior to injection. The hydrolyzed products were identified by using Ultimate 3000 RS Variable Wavelength Detector at 280 nm.

HPLC analysis: Both the esters (D) and (L) BTC-(Phe-OMe)₃ and their gels were performed by taking 20mg samples in 1000 μL solution of miliQ water-acetonitrile (1: 1). Ultimate 3000 RS Variable Wavelength Detector at 280 nm

52.5 FT-IR study:

All reported FT-IR spectra were taken using a Bruker (Tensor 27) FT-IR spectrophotometer. Solid-state measurements were performed with the compounds **1** and **2** using KBr pellet technique with a scan range between 400 and 4000 cm^{-1} over 64 scans at a resolution of 4 cm^{-1} and an interval of 1 cm^{-1} . Further, Again the gel samples were placed between

crystal Zn–Se windows and scanned between 900 to 4000 cm^{-1} over 64 scans at a resolution of 4 cm^{-1} and an interval of 1 cm^{-1}

2.6 Circular dichroism (CD) study:

Secondary structures of both (L) and (D) gels were analyzed with Jasco J-815 Circular Dichroism (CD) spectrometer with the course of dynamic reactions. (L) and (D) gels (17 mmol L^{-1}) were diluted to a final concentration of 5×10^{-5} M in ddH₂O and dTHF (1:1) for experiment and measured from 450 to 200 nm with 0.1 nm data pitch, 20 nm min^{-1} scanning speed, 1 nm bandwidth and 4 s D.I.T.

2.7 Morphological Study

For SEM study, supramolecular gels ((L)-gel and (D)-gel) were placed on a glass slide and coated with gold. Then, micrographs were recorded using a Scanning Electron Microscope (Jeol Scanning Microscope-JSM-7600F). Transmission electron microscopic (TEM) images were taken using a PHILIPS electron microscope (model: CM 200) operated at an accelerating voltage of 200 kV. Both the supramolecular gels (17 mmol L^{-1}) were diluted to 1 mmol L^{-1} in distilled tetrahydrofuran and dried on carbon-coated copper grids (300 mesh) by slow evaporation in air, then allowed to dry separately under vacuum at room temperature.

2.8 Wide angle X-ray diffraction study:

Powder X-ray diffraction studies of compounds **1-2** and corresponding xerogels were performed by placing the samples on the glass plate. Experiments were recorded using Rigaku Smart Lab X-ray diffractometer with a wavelength of 1.5406 Å. X-rays were produced using a sealed tube, and X-ray was detected using a linear counting

detector based on silicon strip technology (Scintillator NaI photomultiplier detector).

2.9 UV-Vis Spectroscopy:

UV-Vis absorption spectra of compounds **1-2** and corresponding gels were recorded using a Varian Cary100 Bio UV-Vis spectrophotometer. All the samples were diluted to 2×10^{-5} M as concentration and UV-Vis spectra were recorded

2.9 Fluorescence Spectroscopy.

Fluorescence spectra of compounds **1-2** and corresponding gels were recorded on a Horiba Scientific Fluoromax 4 spectrometer with 1 cm path length quartz cell at room temperature. The slit width for the excitation and emission spectra was set at 2 nm and 1 nm data pitch

2.10 Rheological measurement and self-healing property:

Mechanical properties of the supramolecular gels ((L)-gel and (D)-gel) were measured using an Anton Paar Physica MCR 301 rheometer with a parallel plate geometry (diameter: 25 mm, gap: 0.5 mm). The temperature was maintained at 25°C using an integrated temperature controller. To determine the mechanical strengths of the supramolecular gels, a dynamic frequency sweep of the self-assembled gels were plotted as a function of frequency in the range 0.05–100 rad/sec with a constant strain value of 0.01%. The stiffness of the self-assembled gels was determined when the storage modulus (G') exceeded the loss modulus (G''). A linear viscoelastic regime (LVR) was performed to determine the exact strain for the experiment at a constant frequency of 10 rad/sec.

The experiments were repeated 3 times with new samples in order to get more precise value for discussion.

Chapter 3: Results and discussion

3.1 Synthesis of the compounds:

Methyl esters of (L) and (D) phenylalanine (Phe) were synthesized and two enantiomeric phenylalanine methyl esters (Phe-OMe) were coupled with benzene-1,3,5-tricarboxylic acid (BTC) by conventional solution phase methodology. Two compounds BTC-(L-Phe-OMe)₃ **1** and BTC-(D-Phe-OMe)₃ **2** were purified and fully characterized by ¹H NMR, ¹³C NMR, FT-IR and mass spectrometry. 17.31 mmol of compounds **1-2** in THF was taken in round bottom flask separately and hydrolysed by 1M LiOH solution. After 1 hour, gel formation was started and completed within 4 hours. Similarly, methyl ester hydrolysis of compounds **1-2** was tried by using 1M KOH and 1M NaOH. However, gel was not formed. Here, counter cations (K⁺ and Na⁺) of corresponding acids play a crucial role for the formation of supramolecular gels.

3.2 HPLC analysis and mass spectrometry:

Product conversion after methyl ester hydrolysis was confirmed by high-performance liquid chromatography (HPLC) and mass spectrometry. Both HPLC and mass spectrometry studies revealed that almost 98% esters were converted into its corresponding acids.

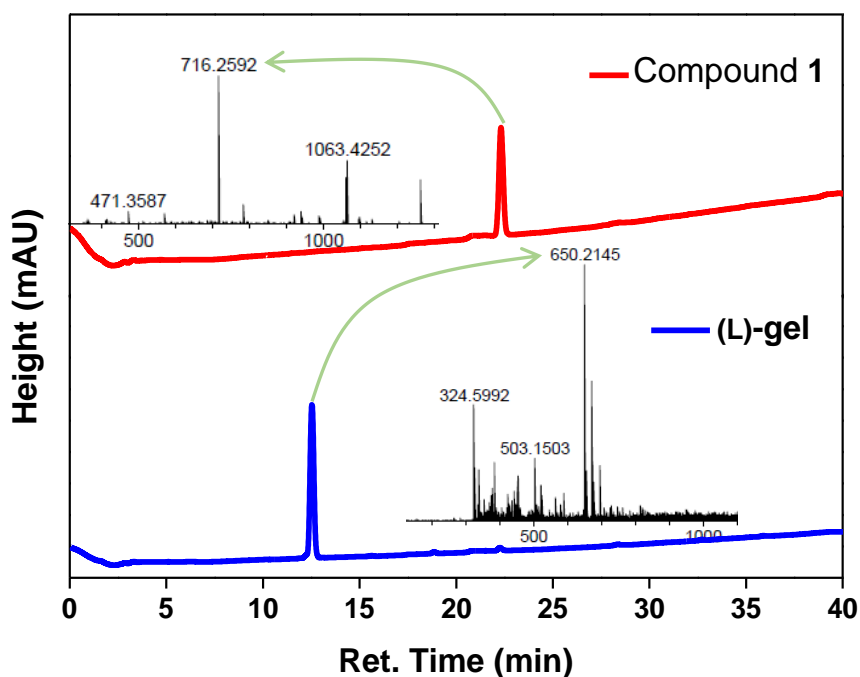


Fig.1: Both mass spectrometry and HPLC analysis show that compound 1 is completely hydrolyzed into acid using LiOH as a base.

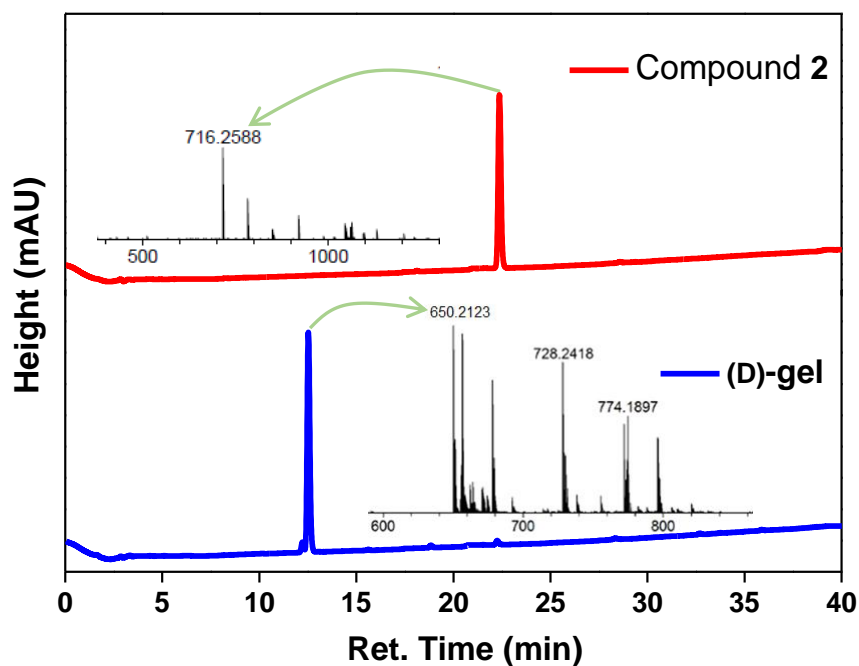


Fig.2: Compound 2 is completely converted into its corresponding acid during hydrolysis

3.3 FT-IR study of gelators and gels:

FTIR spectroscopy was executed in order to investigate the organization of intermolecular H-bonding within the compounds and also to determine the functional groups that are present within the gels and gelators. BTC-(L-Phe-OMe)₃ exhibited N-H bands at 3229, 3061 cm⁻¹, -C=O stretch of amide at 1640 cm⁻¹, amide II band at 1554 cm⁻¹ and ester -C=O band at 1745 cm⁻¹. Whereas BTC-(D-Phe-OMe)₃ displayed N-H stretches at 3234, 3052 cm⁻¹, -C=O stretch of amide at 1640 cm⁻¹, amide II band⁸⁵ at 1556 cm⁻¹ and -C=O stretch of ester at 1744 cm⁻¹. Both the precursor (L) and (D) esters (compounds 1-2) exhibited more than one N-H stretches which indicates that few N-H groups are free and others are hydrogen bonded.⁸⁶ The N-H band along with -C=O

band of amide and amide II band of both the compounds **1-2** had typically been attributed to the presence of threefold intermolecular hydrogen bonding between the neighboring molecules.⁸⁷ N-H stretch of the (L)-gel appeared at 2966 cm^{-1} whereas a peak at 2974 cm^{-1} appeared for N-H stretching vibration of (D)-gel. A red shift of N-H band occurred when gels were produced from their corresponding esters indicating strong self-assembly within the gels. (L)-gel displayed a weak -C=O stretching band at 1640 cm^{-1} and amide II band at 1565 cm^{-1} . (D)-gel also showed -C=O stretch of the amide at 1638 cm^{-1} and amide II band at 1540 cm^{-1} . (L) and (D) gels showed a peak at 1640 cm^{-1} and 1638 cm^{-1} respectively which was attributed to the helical structure at the supramolecular level.⁸⁸ The -C=O stretching bands of the ester groups disappeared when compounds **1-2** formed gels upon hydrolysis.

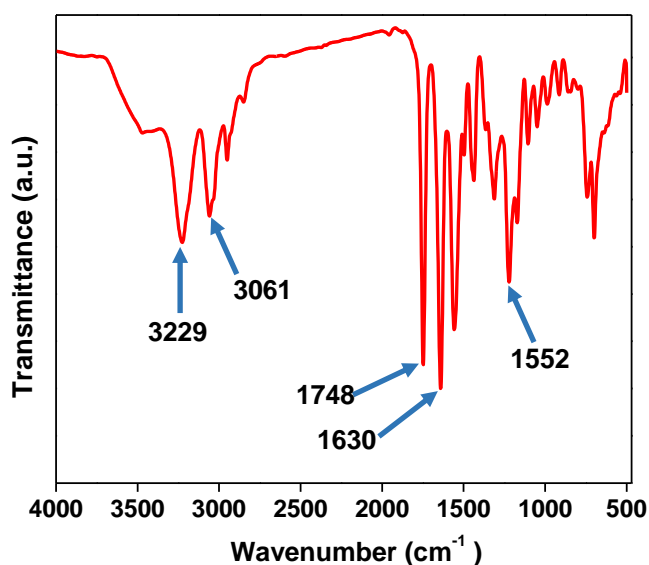


Fig. 3: FT-IR spectrum of compound 1

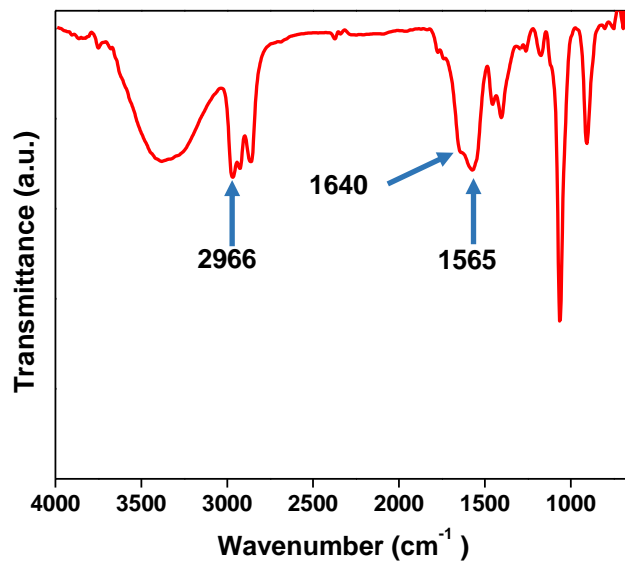


Fig. 4: FT-IR spectrum of (L)-gel

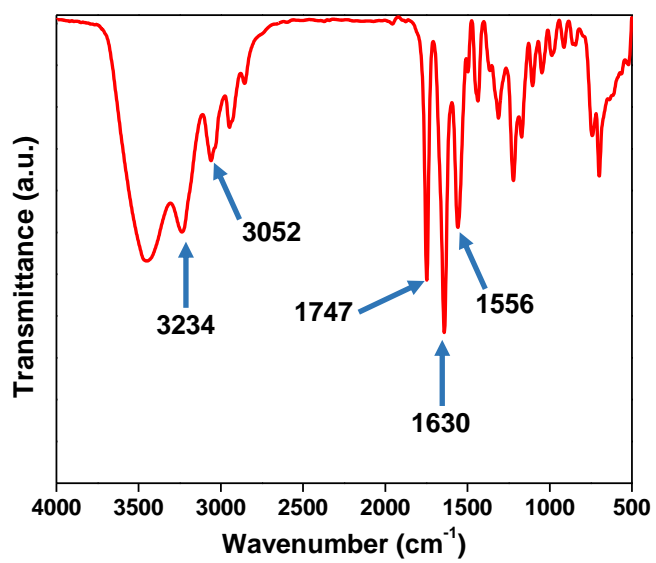


Fig. 5: FT-IR spectrum of compound 2

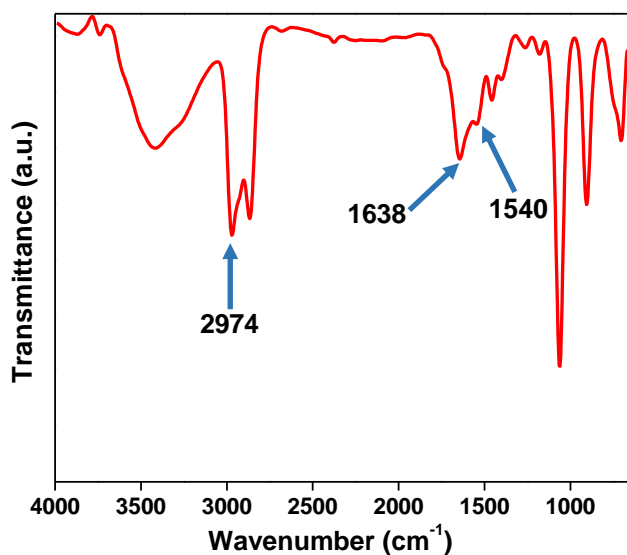


Fig. 6: FT-IR spectrum of (D)-gel

Sr. No.	Compound	N-H stretch	Ester (C=O stretching)	Amide I (C=O stretching)	Amide II (C-N stretching and N-H bending)
1.	Compound 1	3229/ 3061 cm ⁻¹	1748 cm ⁻¹	1630 cm ⁻¹	1552 cm ⁻¹
2.	(L)-gel	2966 cm ⁻¹	--	1640 cm ⁻¹	1565 cm ⁻¹
3.	Compound 2	3234/ 3052 cm ⁻¹	1747 cm ⁻¹	1630 cm ⁻¹	1556 cm ⁻¹
4.	(D)-gel	2974 cm ⁻¹	--	1638 cm ⁻¹	1540 cm ⁻¹

Table 1: FT-IR stretching frequencies of compound 1 and 2 and (L) and (D) gels

3.4 Circular dichroism (CD) study of gels:

Circular dichroism (CD) study was performed in order to investigate the chirality of the self-assembled structures, secondary structure of the gels and co-operativity. CD spectrum exhibited characteristic negative peak at 218 nm for (L)-gel and positive peak at 216 nm for (D)-gel which were attributed to the $n-\pi^*$ transition in amide bonds⁸⁹ Another positive CD signal of the (L)-gel appeared at 243 nm whereas a negative CD signal of the (D)-gel at 248 nm was observed due to the presence of side chain phenylalanine residues.⁹⁰ Circular dichroism spectra of two enantiomeric benzene-tri-carboxamide derivatives showed opposite cotton effects with respect to one another. The chirality of the peripheral side chains induces the core during self-assembly to originate chiral superstructures. The CD signals in the region of 190 nm and 260 nm indicate the helical arrangement of the benzene-1,3,5 tricarboxamide derivatives.⁹¹ Here, chiral helical superstructures were formed for (L)-gel and (D)-gel.

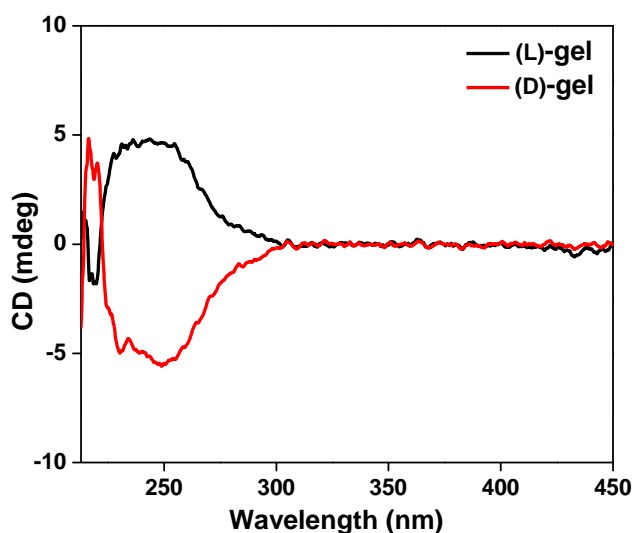
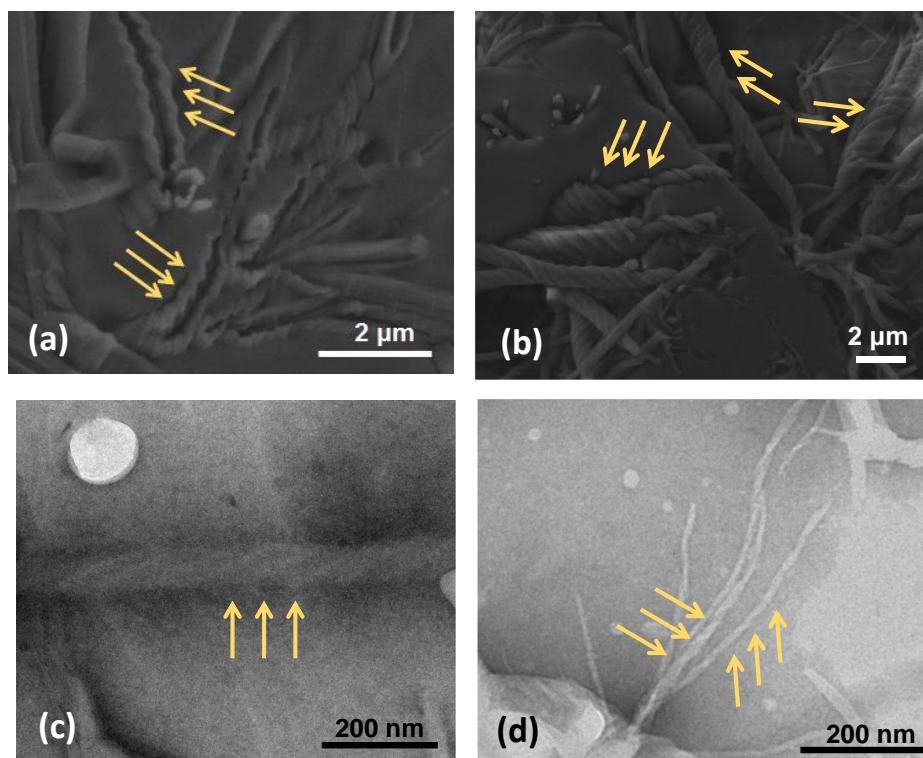


Fig. 7: CD spectra of (L) and (D)-gels

3.5 Morphological study of gels:

The handedness of the self-assembled (L)-gel and (D)-gel was assessed by scanning electron microscopy (SEM) and transmission electron microscopy (TEM). SEM images of self-assembled (L)-gel displayed left handed whereas (D)-gel showed right handed helical structures. TEM images also favored the helicities those were exhibited by SEM. These results suggested that chiral phenylalanine residues play an important role to determine the handedness of the helical structures.



**Fig. 8: a) SEM image of (L)-gel, b) SEM image of (D)-gel,
c) TEM image of (L)-gel and d) TEM image of (D)-gel**

3.6 Wide angle XRD study of gelators and dried gels:

In order to obtain structural information, dried (L) and (D) gels were characterized by power X-ray diffraction (PXRD) technique. The scattering patterns of both the compounds showed a series of characteristics diffraction peaks, which help us to describe different types of self-assembly arising within the gels. Dried (L)-gel displayed a peak at $2\theta = 5.25^\circ$ ($d = 16.81 \text{ \AA}$) and dried (D)-gel showed a characteristic scattering pattern at $2\theta = 5.52^\circ$ ($d = 15.99 \text{ \AA}$) which are attributed due to the circular cross sectional diameter of BTA-Phe moiety.⁹² Other diffraction peaks for (L)-gel at $2\theta = 18.18^\circ$ ($d = 4.87 \text{ \AA}$) and for (D)-gel at $2\theta = 18.10^\circ$ ($d = 4.89 \text{ \AA}$) were the characteristic distance between hydrogen bonded two molecules N (N-H)---C (C=O). The characteristic π - π stacking interactions between the aromatic moieties played a paramount role during the self-assembly, which was revealed from the diffraction peak at $2\theta = 25.30^\circ$ corresponding to the d spacing value 3.51 \AA for (L)-gel and from the diffraction peak at $2\theta = 25.29^\circ$ corresponding to the d spacing value 3.51 \AA for (D)-gel.⁹³

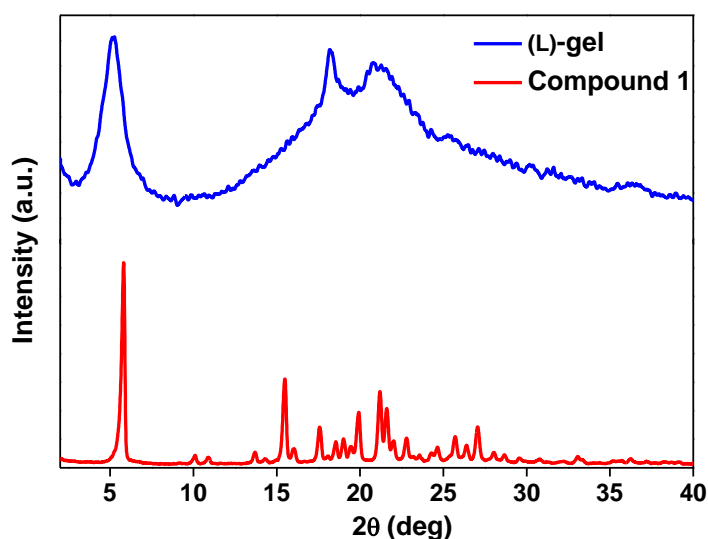


Fig. 9: Wide angle X-ray scattering of the compound 1 and its xerogel

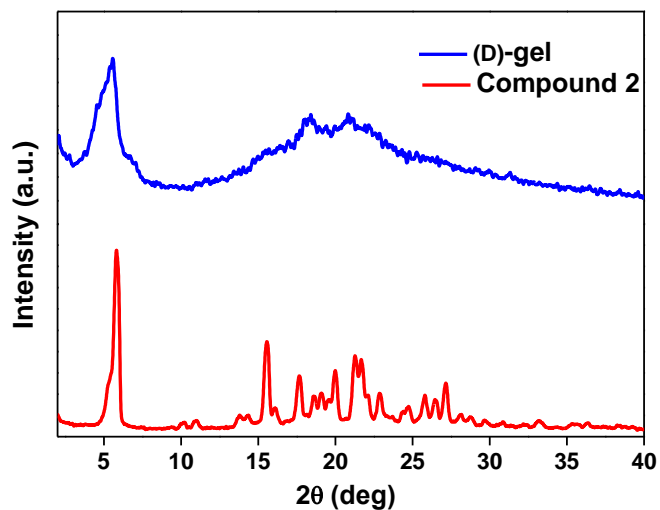


Fig. 10: Wide angle scattering of the compound 2 and its xerogel

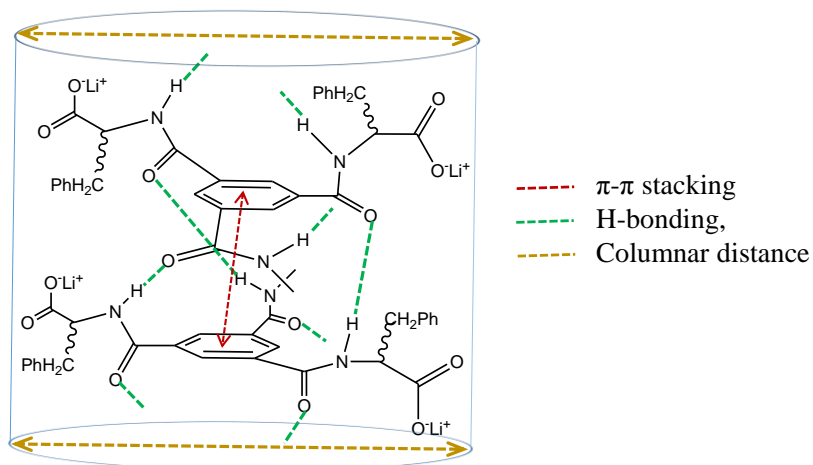


Fig. 11: Proposed self-assembly of the monomeric building blocks to form both the gels

3.7 UV-Vis Spectroscopy of gelators and gels:

To obtain further insights into the intermolecular interactions in supramolecular aggregates and the self-assembly process aided for the formation of gels from precursor compounds, we have recorded UV/Vis spectra of compounds **1-2** and also the corresponding (L) and (D)-gels. UV-Vis spectra of compounds **1-2** showed λ_{\max} at 209 nm which was ascribed from the π - π^* transition of the $-\text{CONH}$ group. A broad shoulder appeared in the region of 225-261 nm which may be attributed to the n - π^* transition of the $-\text{CONH}$ group and π - π^* transition within the side chain phenyl residues. UV-Vis spectra of both the gels showed λ_{\max} at 219 nm and broad shoulder within the range of 235-277 nm. The red shift in UV-Vis spectrum demonstrated the higher order self-assembly in the gel phase materials.

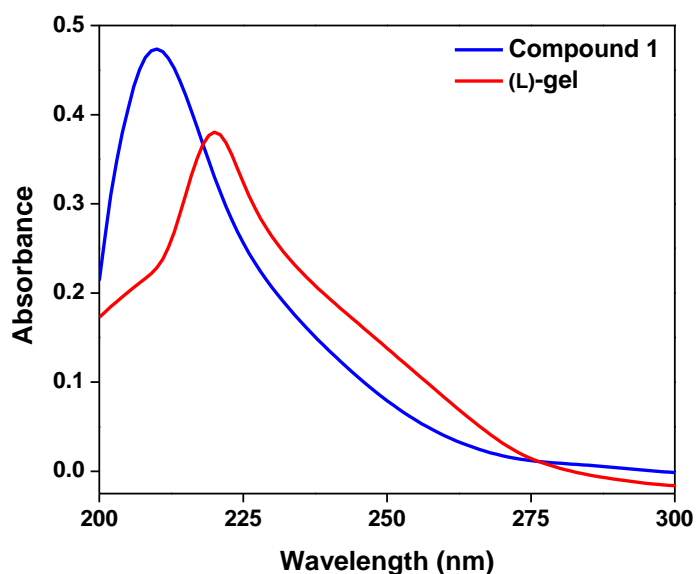


Fig. 12: UV-Visible spectra of compound 1 and it's gel

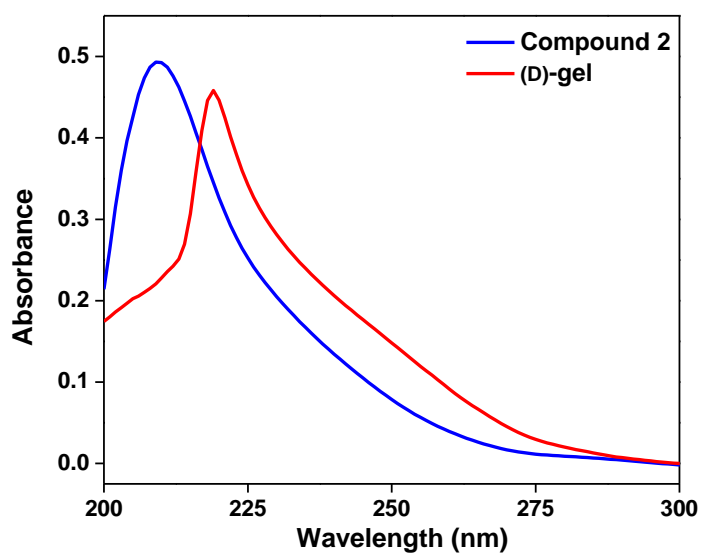


Fig. 13: UV-Visible spectra of the compound 2 and it's gel

3.8 Fluorescence Spectroscopy:

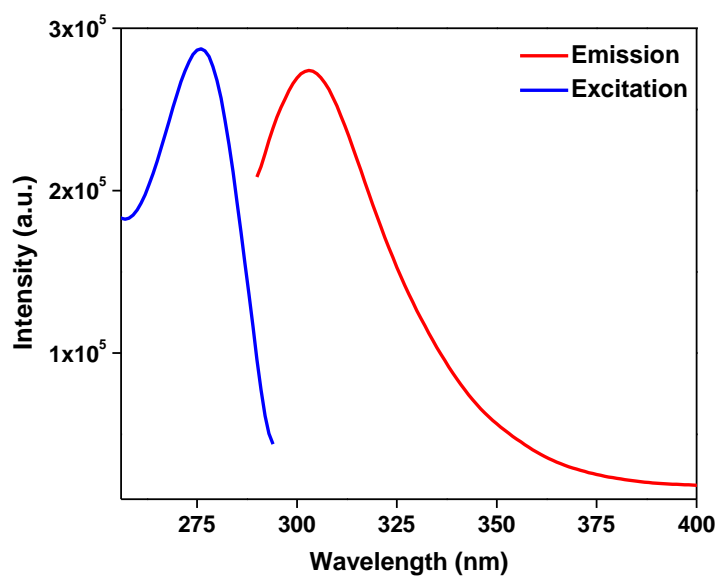


Fig. 14: Emission and excitation spectra of (L)-gel

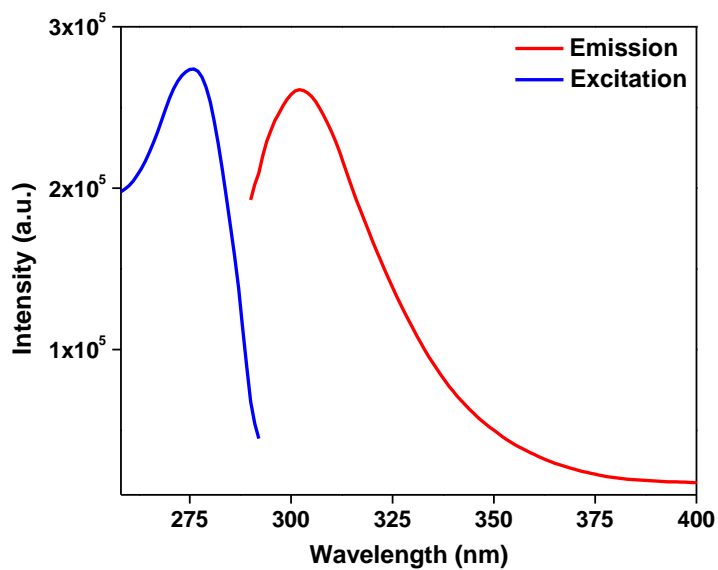


Fig. 15: Emission and excitation spectra of (D)-gel



Fig. 16: Photographic images of (L) and (D)-gels under UV-Visible light

3.9 Rheology study of the gels:

Rheological experiments of (L) and (D) gels were performed to confirm their viscoelastic and mechanical properties. The mechanical strength⁹⁴ and viscoelastic properties of the supramolecular gels designate the

capability power of the gels to entrap the solvent molecules within the three-dimensional molecular network structures which prevents free flow of the solvent. Oscillatory frequency sweep and amplitude sweep experiments were performed to find out the storage and loss moduli (G' and G''). The storage modulus G' represents a solid-like character, which denotes resistance power of the gel to prevent deformation under stress. Whereas the loss modulus G'' indicates the liquid-like behavior that means the inclination of the material to flow. Higher storage modulus (G') value with compare to loss modulus (G'') supports the formation of rigid gels.⁹⁵ Fig.17 and 18 elucidated that storage modulus (G') exceeded the loss modulus (G'') over the oscillating frequency, which favor the formation of a strong and rigid supramolecular gel.⁹⁶ The thixotropic nature of the both supramolecular gels were investigated using a hysteresis loop test. A constant strain of 0.05% was applied (step 1) to both the supramolecular gels at a constant angular frequency of 10 rad s^{-1} . Then, the strain was slowly increased from 0.05% to 30% (step 2) and kept it for 1.67 min. At this high strain, the non-covalent interactions within the supramolecular gels got completely ruptured without affecting the fiber structure of the gels⁹⁷ and as a result gel to sol transition occurred ($G' < G''$). Again, sol to gel transition ($G' > G''$) was observed by applying low strain to 0.05% (step 3) up to 1.67 min due to the reformation of the fibrillar 3D networks. This experiment was performed up to the 9 steps. At the steps 2, 4, 6 and 8, both the gels were destroyed by the application of 30% strain. Whereas at the steps 3, 5, 7 and 9, the strain was decreased from 30% to 0.05% resulting reformation of the gels with 98% recovery of its original stiffness within 1.67 min. The gel recovery behavior is known as self-healing behavior of the gels. The experimental results suggest that in-situ supramolecular polymerization and de-polymerization techniques are responsible for self-healing behavior of the supramolecular gels. In order to verify the self-healing property of the gels, (L) and (D) gels were sliced into two parts and one part was colored with Rhodamine B. Then, two different parts of the supramolecular gel were kept in touch with each other. After 30 minutes, two different parts of each supramolecular (L) and (D) gels

were found to be joined with each other. This is attributed to the presence of numerous hydrogen bonding interactions between the acid/amide functional groups present in the supramolecular gels. The interlinking directional hydrogen bonding involving $-C=O$ and $-OH$ groups of acid and $-NH-$ and $-C=O$ groups of amides, $\pi-\pi$ stacking between the aromatic groups were the responsible factors for this self-healing process.⁹⁸

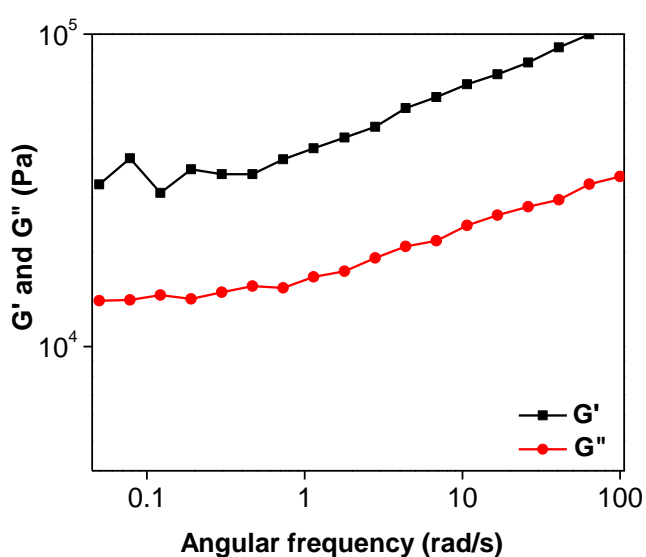


Fig. 17: Dynamic frequency sweep of self-assembled (L)-gel at constant strain 0.01%

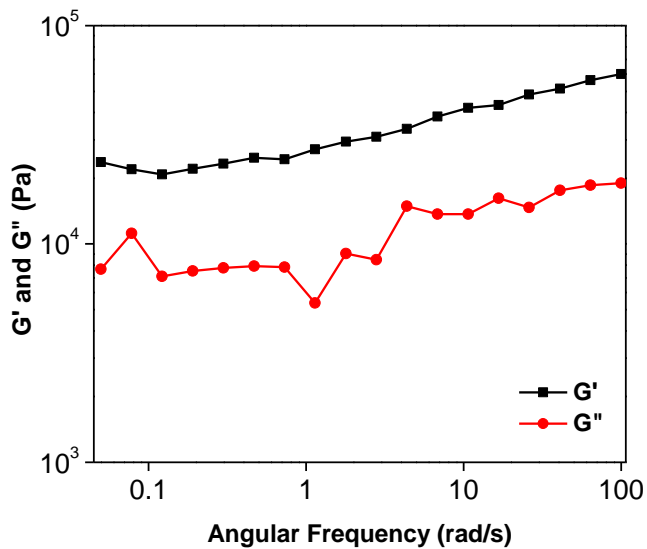


Fig. 18: Dynamic frequency sweep of self-assembled (D)-gel at constant strain 0.01%

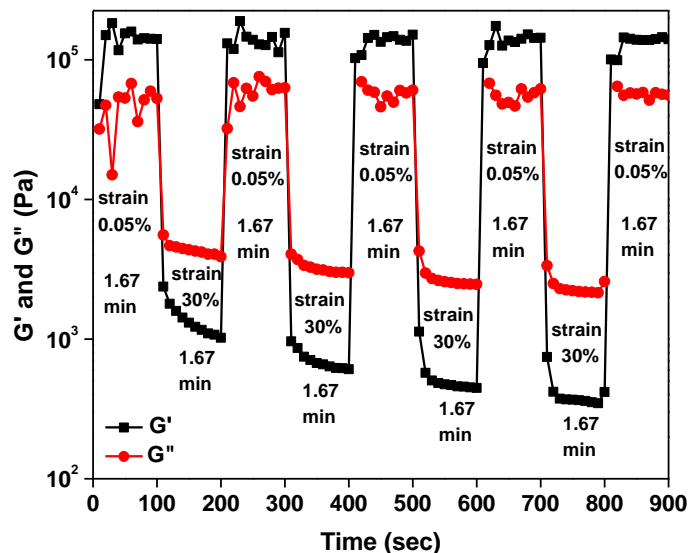


Fig. 19: Hysteresis loop test of self-assembled (L)-gel

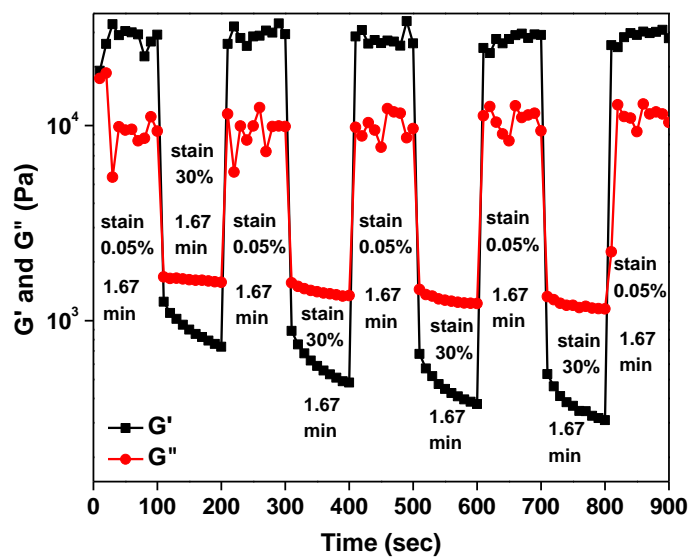


Fig. 20: Hysteresis loop test of self-assembled (D)-gel



Fig. 21: Self-healing behavior of (L)-gel.

3.10. Hydrolysis of compounds by using different bases:

Base	BTC-(L-Phe-OMe) ₃ /Compound 1	BTC-(D-Phe-OMe) ₃ /Compound 2
LiOH	G	G
NaOH	O.S.	O.S.
KOH	O.S.	O.S.

Table 2. Here G-gel, O.S.-opaque solution

3.10.1. Hydrolysis by using LiOH 1(N):



Fig. 22: Both the (D) and (L) compounds form gel during the hydrolysis by using LiOH as a base

3.10.2. Hydrolysis by using NaOH 1(N):



Fig. 23: Both the (D) and (L) compounds form opaque solution during hydrolysis by using NaOH as a base

3.10.3. Hydrolysis by using KOH 1(N):

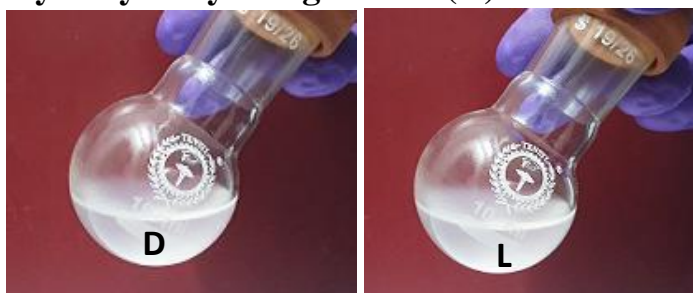


Fig. 24: Both the (D) and (L) compounds form gel opaque solution during hydrolysis by using KOH as a base

Chapter 4: Conclusion

In this work, we have prepared in situ (L) and (D) gels by hydrolyzing corresponding (L) and (D) esters. The role of counter cations of hydrolyzed acids for the formation of supramolecular gels were also assessed. Here smaller size of Li^+ allowed the fibers to self-assemble into helical superstructure whereas the larger size of Na^+ and K^+ ions resist the fibers to self-assemble into helical superstructure. FT-IR and PXRD studies revealed that hydrogen bonding and π - π stacking interactions were responsible for the formation of gels. Rheological measurements showed self-healing behavior of the gels. Circular dichroism, TEM and SEM images revealed that peripheral chiral amino acids attached with benzene-1,3,5-tricarboxylic acid induced helical superstructure. (L)-phenylalanine derived gel induced left handed as well as (D)-phenylalanine derived gel induced right handed helical superstructures. Here, phenylalanine acts as chiral dopant and helps to induce the chirality within the supramolecular system. A unidirectional three folded hydrogen bond is formed due to the self-assembly of peripheral side chains of benzene-tri-carboxamide which apparently locks the building block units on the top of each other and thereby forms columnar stacks. The unidirectional nature of the hydrogen bonds, depending upon the chirality of the peripheral units, acts as trigger to tune the handedness of helicity at supramolecular level.

Appendix A

^1H NMR, ^{13}C NMR and Mass spectrometry of compounds:

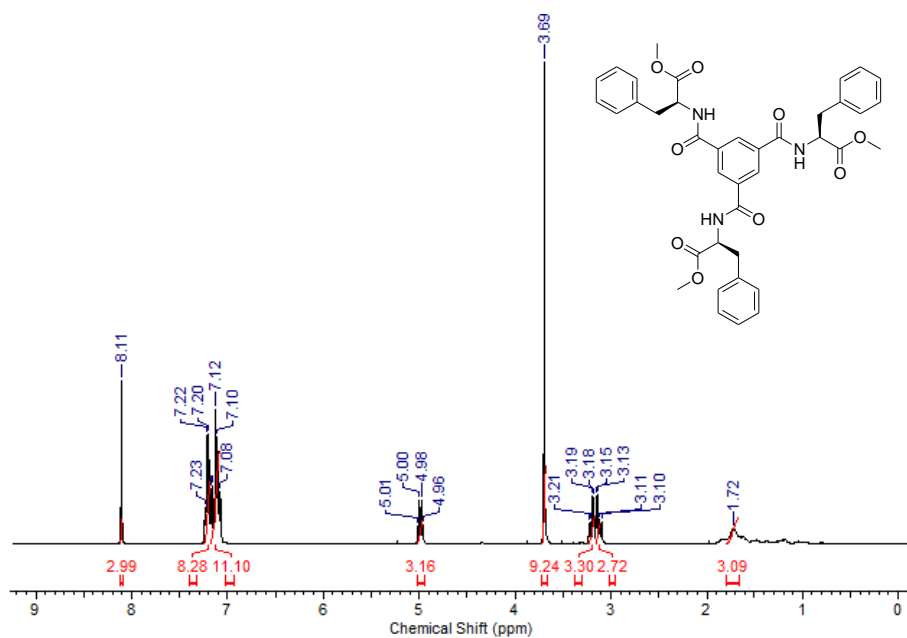


Fig. 25: 400 MHz ^1H NMR spectrum of compound 1 in CDCl_3

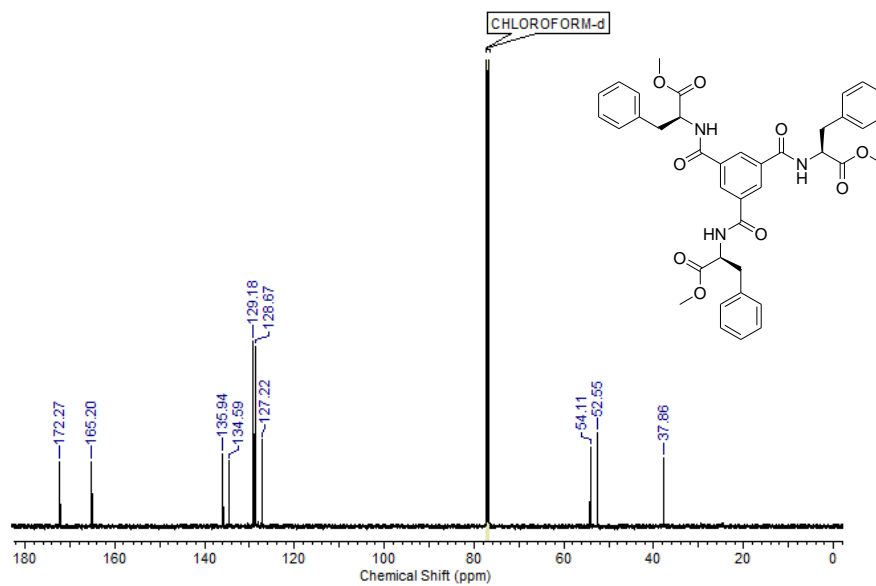


Fig. 26: 100 MHz ^{13}C NMR spectrum of compound 1 in CDCl_3

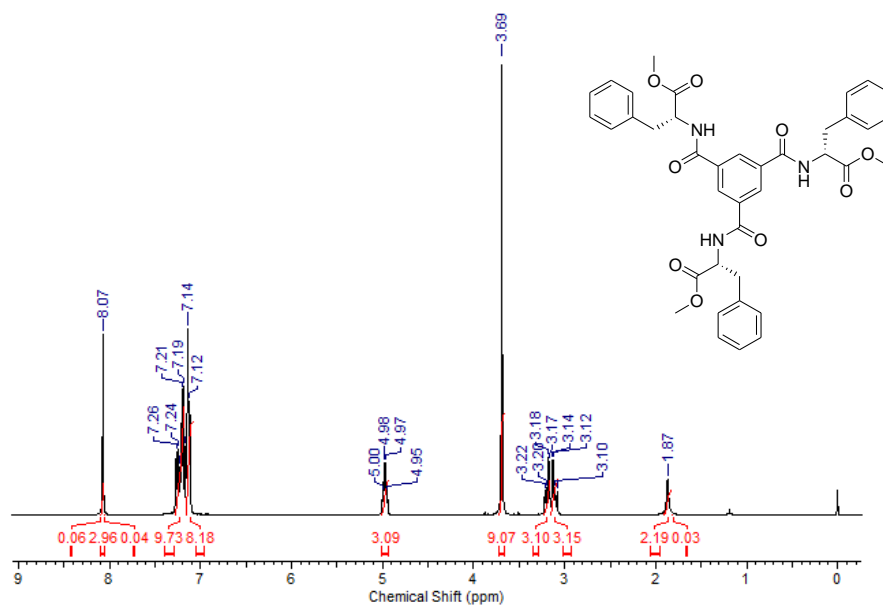


Fig. 27: 400 MHz ^1H NMR spectrum of compound 2 in CDCl_3

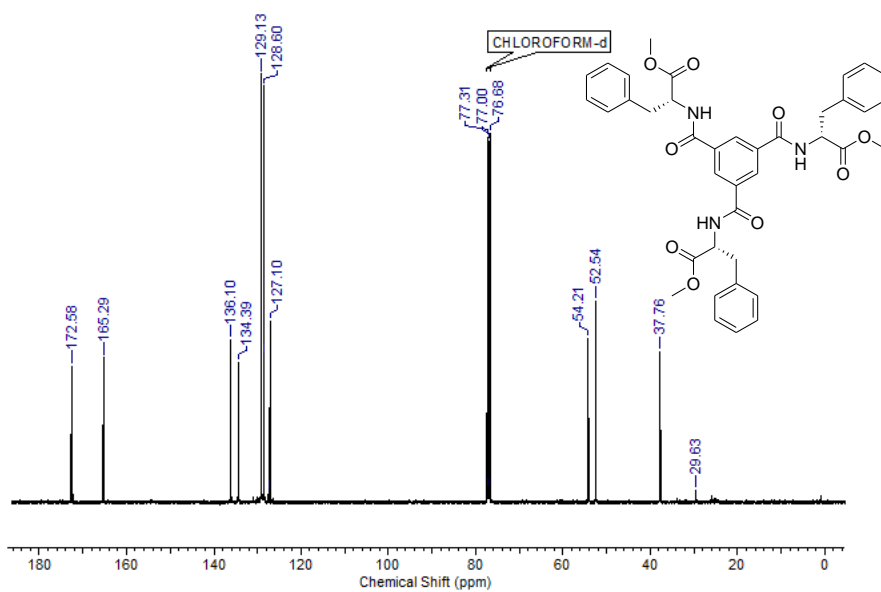


Fig. 28: 100 MHz ^{13}C NMR spectrum of compound 1 in CDCl_3

Mass spectrometry:

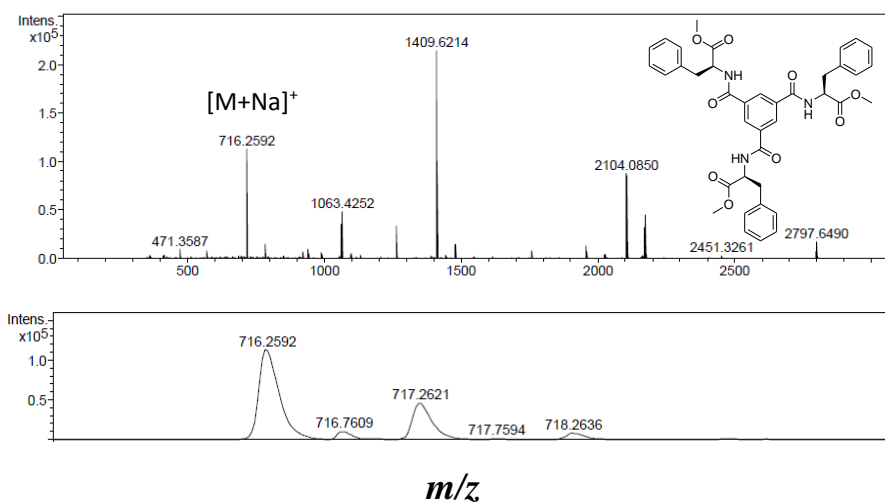


Fig. 29: ESI-MS spectrum of compound 1

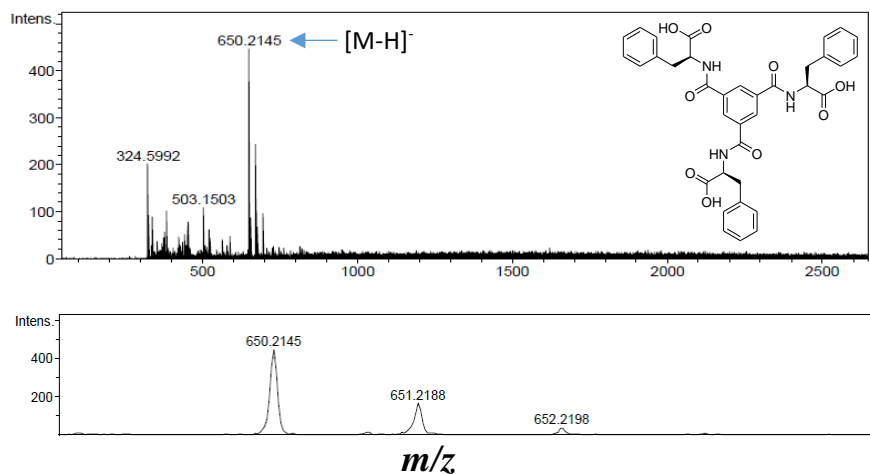


Fig. 30: ESI-MS spectrum of (L)-gel

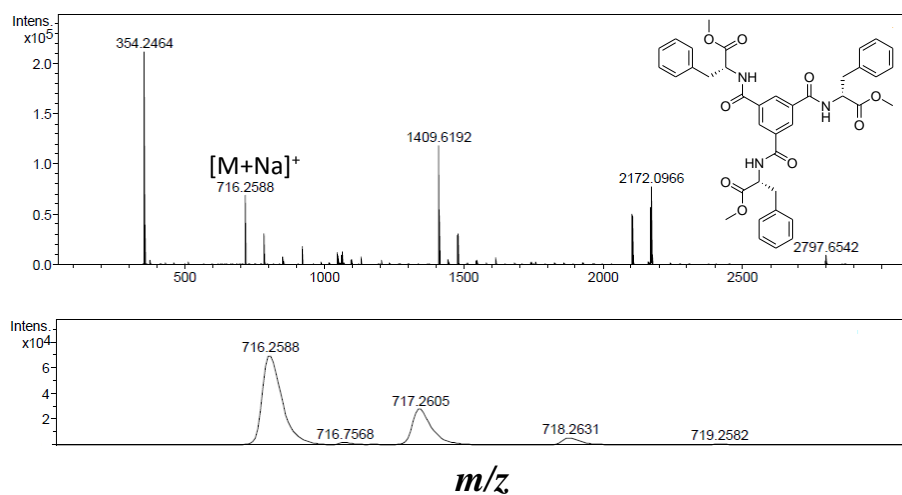


Fig. 31: ESI-MS spectrum of compound 2

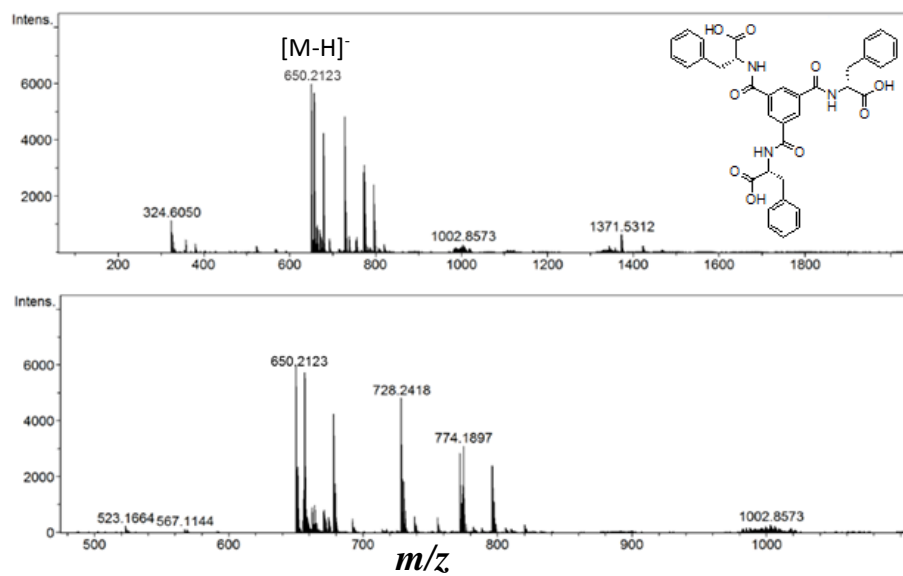


Fig. 32: ESI-MS spectrum of (D)-gel

References:

1. C. C. Lee, C. Grenier, E. W. Meijer and A. P. H. J. Schenning, Preparation and characterization of self-assembled nanofibers, *Chem. Soc. Rev.*, **2009**, *38*, 671-683.
2. J. Crassous, Chiral transfer in coordination complexes: towards molecular materials, *Chem. Soc. Rev.*, **2009**, *38*, 830-845
3. L. A. E. and A. D. Hamilton, Water Gelation by Small Organic Molecules, *Chem. Rev.*, **2004**, *104*, 1201-1218.
4. O. Gronwald, E Snip, S. Shinkai, Gelators for organic liquids based on self-assembly: a new facet of supramolecular and combinatorial chemistry, *Current Opinion in Colloid and Interface Science*, **2002**, *7*, 148-156
5. N. M. Sangeetha, U. Maitra, Supramolecular gels: Functions and uses, *Chem. Soc. Rev.*, **2005**, *34*, 821-836.
6. L. Zhang, X. Wang, T. Wang, and M. Liu, Tuning Soft Nanostructures in Self-assembled Supramolecular Gels: From Morphology Control to Morphology-Dependent Functions. *Small*, **2015**, *11*, 1025-1038.
7. J. S. Seo, D. Whang, H. Lee, S. I. Jun, J. Oh, Y. J. Jeon, K. Kim, A homochiral metal-organic porous material for enantioselective separation and catalysis, *Nature*, **2000**, *404*, 982-986
8. S. Nimri, E. Keinan, Antibody-Metalloporphyrin Catalytic Assembly Mimics Natural Oxidation Enzymes, *J. Am. Chem. Soc.*, **1999**, *121*, 8978-8982.
9. T. Verbiest, S. V. Elshocht, M. Kauranen, L. Hellemans, J. Snauwaert, C. Nuckolls, T. J. Katz, A. Persoons, Strong enhancement of nonlinear optical properties through supramolecular chirality, *Science*, **1998**, *282*, 913-915

10. S. K. Jha, K. S. Cheon, M. M. Grenn, J. V. Selinger, Chiral Optical Properties of a Helical Polymer Synthesized from Nearly Racemic Chiral Monomers Highly Diluted with Achiral Monomers, *J. Am. Chem. Soc.*, **1999**, *121*, 1665-1673
11. K. Akagi, G. Piao, S. Kaneko, K. Sakamaki, H. Shirakawa, M. Kyotani, Helical Polyacetylene Synthesized with a Chiral Nematic Reaction Field, *Science*, **1998**, *282*, 1683-1686
12. E. Yashima, K. Maeda, Y. Okamoto, Memory of macromolecular helicity assisted by interaction with achiral small molecules, *Nature*, **1999**, *399*, 449-451
13. H. Ogoshi, T. Mizutani, Multifunctional and Chiral Porphyrins: Model Receptors for Chiral Recognition, *Acc. Chem. Res.* **1998**, *31*, 81-89
14. L. J. Prins, J. Huskens, F. Jong, P. Timmerman, D. N. Reinhoudt, Complete asymmetric induction of supramolecular chirality in a hydrogen-bonded assembly, *Nature*, **1999**, *398*, 498-502
15. Y. Furusho, T. Kimura, Y. Mizuno, T. Aida, Chirality-Memory Molecule: A D_2 -Symmetric Fully Substituted Porphyrin as a Conceptually New Chirality Sensor, *J. Am. Chem. Soc.*, **1997**, *119*, 5267-5268
16. E. M. Geertsema, Chiroptical Molecular Switches, *Chem. Rev.* **2000**, *100*, 1789-1816
17. S. Zahn, J. W. Canary, Electron-Induced Inversion of Helical Chirality in Copper Complexes of *N,N*-Dialkylmethionines, *Science*, **2000**, *288*, 1404-1407
18. G. Baum, E. C. Constable, D. Fenske, C. E. Housecroft, T. Kulke, Stereoselective Double-Helicate Assembly from Chiral 2,2':6',2'':6'',2'''-Quaterpyridines and Tetrahedral Metal Centres, *Chemistry A European Journal*, **1999**, *5*, 1862-1873
19. X. Huang, B. H. Rickman, B. Borhan, N. Berova, K. Nakanishi, Zinc Porphyrin Tweezer in Host-Guest Complexation: Determination of Absolute Configurations of Diamines, Amino Acids, and Amino

Alcohols by Circular Dichroism, *J. Am. Chem. Soc.* **1998**, *120*, 6185-6186

20. E. Yashima, T. Matsushima, Y. Okamoto, Chirality Assignment of Amines and Amino Alcohols Based on Circular Dichroism Induced by Helix Formation of a Stereoregular Poly((4-carboxyphenyl)acetylene) through Acid–Base Complexation, *J. Am. Chem. Soc.*, **1997**, *199*, 6345-6359

21. Y. Oiu, P. Chen, P. Gua, Y. Li, M. Liu, Supramolecular Chiroptical Switches Based on Achiral Molecules, *Advanced Materials*, **2008**, *20*, 2908-2913

22. Y. Xu, H. Jiang, Q. Zhang, F. Wang, G. Zou, Helical polydiacetylene prepared in the liquid crystal phase using circular polarized ultraviolet light, *Chem Commun*, **2014**, *50*, 365-367

23. Y. Xu, G. Yang, H. Xia, G. Zou, Q. Zhan, J. Gao, Enantioselective synthesis of helical polydiacetylene by application of linearly polarized light and magnetic field, *Nat. Commun.*, **2014**, *5*, 5050

24. Z. Shen, T. Wang, M. Liu, Macroscopic Chirality of Supramolecular Gels Formed from Achiral Tris (ethyl cinnamate) Benzene-1,3,5-tricarboxamides, *Angew. Chem. Int. Ed.*, **2014**, *53*, 13424-13428

25. Y. Li, T. Wang, M. Liu, Gelating-induced supramolecular chirality of achiral porphyrins: chiroptical switch between achiral molecules and chiral assemblies, *Soft Matter*, **2007**, *3*, 1312-1317

26. L. Zhang, L. Qin, X. Wang, H. Cao, M. Liu, Supramolecular Chirality in Self-Assembled Soft Materials: Regulation of Chiral Nanostructures and Chiral Functions, *Adv. Mater.*, **2014**, *26*, 6959 - 6964

27. L. Zhang, X. Wang, T. Wang, M. Liu, Tuning Soft Nanostructures in Self-assembled Supramolecular Gels: From Morphology Control to Morphology-Dependent Functions, *Small*, **2015**, *11*, 1025 – 1038

28. X. Zhu, P. Duan, L. Zhang and M. Liu, Regulation of the Chiral Twist and Supramolecular Chirality in Co-Assemblies of Amphiphilic L-Glutamic Acid with Bipyridines, *Chem. – Eur. J.*, **2011**, *17*, 3429-3437

29. C. Liu, Q. Jin, K. Lv, L. Zhang and M. Liu, Water tuned the helical nanostructures and supramolecular chirality in organogels, *Chem. Commun.*, **2014**, 50, 3702-3705
30. X. Wang, P. Duan, M. Liu, Universal chiral twist *via* metal ion induction in the organogel of terephthalic acid substituted amphiphilic L-glutamide, *Chem. Commun.*, **2012**, 48, 7501-7503
31. X. Wang, P. Duan, M. Liu, Self-Assembly of π -Conjugated Gelators into Emissive Chiral Nanotubes: Emission Enhancement and Chiral Detection, *Chem. – Asian J.*, **2014**, 9, 770-8.
32. A. Noro, M. Hayashi, Y. Matasushita, Design and properties of supramolecular polymer gels, *Soft Matter*, **2012**, 8, 6416-6429
33. T. Tu, X. L. Bao, W. Assenmacher, H. Peterlik, J. Daniels, K. H. Dotz, Efficient Air-Stable Organometallic Low-Molecular-Mass Gelators for Ionic Liquids: Synthesis, Aggregation and Application of Pyridine-Bridged Bis(benzimidazolylidene)-Palladium Complexes, *Chem. Eur. J.*, **2009**, 15, 1853-1861
34. M. Suzuki, M. Yumoto, H. Shirai, K. Hanabusa, Supramolecular Gels Formed by Amphiphilic Low-Molecular-Weight Gelators of N^{α}, N^{ϵ} -Diacyl-L-Lysine Derivatives, *Chem. Eur. J.* **2008**, 14, 2133-2144
35. J. K. H. Hui, Z. Yu, M. J. MacLachlan, Supramolecular Assembly of Zinc Salphen Complexes: Access to Metal-Containing Gels and Nanofibers, *Angew. Chem. Int. Ed.*, **2007**, 46, 7980-7983
36. A. Gopal, M. Hifsudheen, S. Furumi, M. Takeuchi, A. Ajayaghosh, Thermally Assisted Photonic Inversion of Supramolecular Handedness, *Angew. Chem. Int. Ed.* **2012**, 51, 10505-10661
37. S. R. Nam, H. Y. Lee, J. I. Hong, S. R. Nam, H. Y. Lee, J. I. Hong, Control of Macroscopic Helicity by Using the Sergeants-and-Soldiers Principle in Organogels, *Chem. Eur. J.*, **2008**, 14, 6040-6043
38. A. Y. Tam, K. M. Wong, V. W. Yam, Influence of Counter anion on the Chiral Supramolecular Assembly of Alkynyl platinum(II)

Terpyridyl Metallogels That Are Stabilised by Pt···Pt and π - π Interactions, *Chem. Eur. J.* **2009**, *15*, 4775-4778

39. N. Shi, G. Yin, H. Li, M. Han, Z. Xu, Uncommon hexagonal microtubule based gel from a simple trimesic amide, *New J. Chem.*, **2008**, *32*, 2011-2015

40. X. Zhu, Y. Li, P. Duan, M. Liu, Self-Assembled Ultralong Chiral Nanotubes and Tuning of Their Chirality Through the Mixing of Enantiomeric Components, *Chem. Eur. J.*, **2010**, *16*, 8034-8040

41. Q. Jin, L. Zhang, M. Liu, Solvent-Polarity-Tuned Morphology and Inversion of Supramolecular Chirality in a Self-Assembled Pyridylpyrazole-Linked Glutamide Derivative: Nanofibers, Nanotwists, Nanotubes, and Microtubes, *Chem. Eur. J.*, **2013**, *19*, 9234-9241

42. Z. Shen, T. Wang and M. Liu, Macroscopic Chirality of Supramolecular Gels Formed from Achiral Tris (ethyl cinnamate) Benzene-1, 3, 5-tricarboxamides, *Angew. Chem., Int. Ed.*, **2014**, *53*, 13424-13428

43. J. Cui, A. Liu, Y. Guan, J. Zheng, Z. Shen, X. Wan, Tuning the Helicity of Self-Assembled Structure of a Sugar-Based Organogelator by the Proper Choice of Cooling Rate, *Langmuir.*, **2010**, *26*, 3615-3622

44. P. Duan, L. Qin, X. Zhu, M. Liu, Hierarchical Self-Assembly of Amphiphilic Peptide Dendrons: Evolution of Diverse Chiral Nanostructures Through Hydrogel Formation Over a Wide pH Range, *Chem. Eur. J.*, **2011**, *17*, 6389-6395

45. B. Verdejo, F. Rodriguez-Llansola, B. Escuder, J. F. Miravet, P. Ballester, Sodium and pH responsive hydrogel formation by the supramolecular system calix[4]pyrrole derivative /tetramethylammonium cation, *Chem. Commun.*, **2011**, *47*, 2017-2019

46. J. Wu, T. Yi, T. Shu, M. Yu, Z. Zhou, M. Xu, Y. Zhou, H. Zhang, J. Han, F. Li, C. Huang, Ultrasound Switch and Thermal Self-Repair of

Morphology and Surface Wettability in a Cholesterol-Based Self-Assembly System, *Angew. Chem. Int. Ed.*, **2008**, *47*, 1063–1067

47. R. Wang, X. Liu, J. Li, Engineering Molecular Self-Assembled Fibrillar Networks by Ultrasound, *Cryst. Growth Des.* **2009**, *9*, 3286–3291

48. G. Cravotto, P. Cintas, Molecular self-assembly and patterning induced by sound waves. The case of gelation, *Chem. Soc. Rev.*, **2009**, *38*, 2684–2697

49. S. Kawano, N. Fujita, S. Shinka, A Coordination Gelator That Shows a Reversible Chromatic Change and Sol–Gel Phase-Transition Behavior upon Oxidative/Reductive Stimuli, *J. Am. Chem. Soc.*, **2004**, *126*, 8592–8593

50. V. Caplar, L. Frkanec, N. S. Vujcic, M. Zinic, Positionally Isomeric Organic Gelators: Structure–Gelation Study, Racemic versus Enantiomeric Gelators, and Solvation Effects, *Chem. Eur. J.*, **2010**, *16*, 3066–3082

51. M. Bielejewski, A. Lapinski, R. Luboradzki, J. Tritt-Goc, Solvent Effect on 1,2-*O*-(1-Ethylpropylidene)- α -D-glucofuranose Organogel Properties, *Langmuir*, **2009**, *25*, 8274–8279

52. M. Bielejewski, A. Lapinski, R. Luboradzki, J. Tritt-Goc, Influence of solvent on the thermal stability and organization of self-assembling fibrillar networks in methyl-4,6-*O*-(*p*-nitrobenzylidene)- α -D-glucopyranoside gels, *Tetrahedron*, **2011**, *67*, 7222–7230

53. W. Edwards, C. A. Lagadec, D. K. Smith, Solvent–gelator interactions-using empirical solvent parameters to better understand the self-assembly of gel-phase materials, *Soft Matter*, **2011**, *7*, 110–117

54. T. L. Greaves, A. Weerawardena, C. J. Drummond, Nanostructure and amphiphile self-assembly in polar molecular solvents: amides and the “solvophobic effect”, *Phys. Chem. Chem. Phys.*, **2011**, *13*, 9180–9186

55. D. J. van Dijken, J. M. Beierle, M. C. Stuart, W. Szymanski, W. R. Browne and B. L. Feringa, Autoamplification of Molecular Chirality through the Induction of Supramolecular Chirality, *Angew. Chem., Int. Ed.*, **2014**, *53*, 5073-5077
56. A. T. Haedler, S. C. Meskers, R. H. Zha, M. Kivala, H. W. Schmidt and E. W. Meijer, Pathway Complexity in the Enantioselective Self-Assembly of Functional Carbonyl-Bridged Triarylamine Trisamides, *J. Am. Chem. Soc.*, **2016**, *138*, 10539-10545
57. M. M. J. Smulders, A. P. H. J. Schenning and E. W. Meijer, Insight into the Mechanisms of Cooperative Self-Assembly: The “Sergeants-and-Soldiers” Principle of Chiral and Achiral C₃-Symmetrical Discotic Triamides, *J. Am. Chem. Soc.*, **2008**, *130*, 606-611
58. J. Gestel, A. R. A. Palmans, B. Titulaer, J. A. J. M. Vekemans and E. W. Meijer, “Majority-Rules” Operative in Chiral Columnar Stacks of C₃-Symmetrical Molecules, *J. Am. Chem. Soc.*, **2005**, *127*, 5490-5494
59. G. Liu, D. Zhang and C. Feng, Control of Three-Dimensional Cell Adhesion by the Chirality of Nanofibers in Hydrogels, *Angew. Chem., Int. Ed.*, **2014**, *53*, 7789-7793
60. K. Lv, L. Zhang, W. Lu and M. Liu, Control of Supramolecular Chirality of Nanofibers and Its Effect on Protein Adhesion, *ACS Appl. Mater. Interfaces*, **2014**, *6*, 18878-18884
61. J. H. Jung, M. Masuda, T. Shimizu and S. Shinkai, Helical Ribbon Aggregate Composed of a Crown-Appended Cholesterol Derivative Which Acts as an Amphiphilic Gelator of Organic Solvents and as a Template for Chiral Silica Transcription, *J. Am. Chem. Soc.*, **2001**, *123*, 8785-8789
62. J. H. Jung, H. Kobayashi, K. J. C. Bommel, S. Shinkai and T. Shimizu, Creation of Novel Helical Ribbon and Double-Layered Nanotube TiO₂ Structures Using an Organogel Template, *Chem. Mater.*, **2002**, *14*, 1445-1447

63. F. Rodríguez-Llansola, B. Escuder and J. F. Miravet, Switchable Performance of an L-Proline-Derived Basic Catalyst Controlled by Supramolecular Gelation, *J. Am. Chem. Soc.*, **2009**, *131*, 11478-11484
64. Y. Yang, M. Suzuki, H. Fukui, H. Shirai and K. Hanabusa, Preparation of Helical Mesoporous Silica and Hybrid Silica Nanofibers Using Hydrogelator, *Chem. Mater.*, **2006**, *18*, 1324-1329
65. G.Liu, L.Y. Zhu, W. Ji, C. L. Feng, Z. X. Wei, Inversion of the Supramolecular Chirality of Nanofibrous Structures through Co-Assembly with Achiral Molecules, *Angew. Chem. Int. Ed.* **2016**, *55*, 2411-2415.
66. X. Ran, P. Zhang, S. Qu, H. Wang, B. Bai, H. Liu, C. Zhao, M. Li, Solvent-Induced Helix Superstructure in Achiral Dumbbell-Shaped Hydrazine Derivatives, *Langmuir*, **2011**, *27*, 3945-3951
67. P. Xue, Y. Zhang, J. Jia, D. Xu, X. Zhang, X. Liu, H.Zhou, P. Zhang, R. Lu, M. Takafuji, H. Ihara, Solvent-dependent photophysical and anion responsive properties of one glutamide gelator, *Soft Matter*, **2011**, *7*, 8296-8304
68. P. Xue, R. Lu, X. Yang, L. Zhao, D. Xu, Y. Liu, H.Zhang, H. Nomoto, M. Takafuji, H. Ihara, Self-Assembly of a Chiral Lipid Gelator Controlled by Solvent and Speed of Gelation, *Chem. Eur. J.*, **2009**, *15*, 9824-9835
69. Y. Jeong, K. Hanabusa, H. Masunaga, I. Akiba, K.Miyoshi, S. Sakurai, K. Sakurai, Solvent/Gelator Interactions and Supramolecular Structure of Gel Fibers in Cyclic Bis-Urea/Primary Alcohol Organogels, *Langmuir*, **2005**, *21*, 586-594
70. E. Yashima, K. Maeda, H. Iida, Y. Furusho, K. Nagai, Helical Polymers: Synthesis, Structures, and Functions, *Chem. Rev.*, **2009**, *109*, 6102-6211

71. Y. Kamikawa and T. Kato, Color-Tunable Fluorescent Organogels: Columnar Self-Assembly of Pyrene-Containing Oligo(glutamic acid)s, *Langmuir*, **2007**, *23*, 274-278
72. X. F. Wang, P. F. Duan and M. H. Liu, Universal chiral twist *via* metal ion induction in the organogel of terephthalic acid substituted amphiphilic L-glutamide, *Chem. Commun.*, **2012**, *48*, 7501-7503
73. W. Miao, D. Yang, M. Liu, Multiple-Stimulus-Responsive Supramolecular Gels and Regulation of Chiral Twists: The Effect of Spacer Length, *Chem-European Journal*, **2015**, *21*, 7562-7570
74. J. Qingxian, L. Jing, L. Xiaogang, Z. Li, F. Shaoming, L. Minghua, Function and Application of Supramolecular Gels: Chiral Molecular Recognition and Asymmetric Catalysis, *Progress in Chemistry*, **2014**, *26*, 919-930
75. M. M. J. Smulders, A. P. H. J. Schenning and E. W. Meijer, Insight into the Mechanisms of Cooperative Self-Assembly: The “Sergeants-and-Soldiers” Principle of Chiral and Achiral C₃-Symmetrical Discotic Triamides, *J. Am. Chem. Soc.*, **2008**, *130*, 606-611
76. G. Liu, J. Liu, C. Feng and Y. Zhao. Unexpected right-handed helical nanostructures co-assembled from L-phenylalanine derivatives and achiral bipyridines. *Chem. Sci.*, **2017**, *8*, 1769-1775
77. A. Friggeri, C. Pol, K. J. C. van Bommel, A. Heeres, M. C. A. Stuart, B. L. Feringa and J. Esch, Cyclohexane-Based Low Molecular Weight Hydrogelators: A Chirality Investigation, *Chem.–Eur. J.*, **2005**, *11*, 5353-5361
78. B. W. Messmore, P. A. Sukerkar and S. I. Stupp, Mirror Image Nanostructures, *J. Am. Chem. Soc.*, **2005**, *127*, 7992-7993
79. C. Li, Z. Tang and L. Jiang, Twisted Metal–Amino Acid Nanobelts: Chirality Transcription from Molecules to Frameworks, *J. Am. Chem. Soc.*, **2010**, *132*, 8202-8209
80. E. Yashima and K. Maeda, Chirality-Responsive Helical Polymers, *Macromolecules*, **2008**, *41*, 3-12

- 81.** Y. Yan, Z. Yu, Y. W. Huang, W. X. Yuan, Z. X. Wei, Helical Polyaniline Nanofibers Induced by Chiral Dopants by a Polymerization Process, *Adv. Mater.*, **2007**, *19*, 3353-3357
- 82.** Q. Li, L. Green, N. Venkataraman, I. Shiyanovskaya, A. Khan, A. Urbas, J. W. Doane, Reversible Photoswitchable Axially Chiral Dopants with High Helical Twisting Power, *J. Am. Chem. Soc.*, 2007, *129*, 12908-12909
- 83.** M. Wang, P. Zhou, J. Wang, Y. Zhao, H. Ma, J. R. Lu, H. Xu, Left or Right: How Does Amino Acid Chirality Affect the Handedness of Nanostructures Self-Assembled from Short Amphiphilic Peptides?, *J. Am. Chem. Soc.*, **2017**, *139*, 4185-4194
- 84.** M. Liu, L. Zhang and T. Wang, Supramolecular Chirality in Self-Assembled Systems, *Chem. Rev.*, **2015**, *115*, 7304-7397.
- 85.** Z. Shen, T. Wang, M. Liu, Macroscopic Chirality of Supramolecular Gels Formed from Achiral Tris(ethyl cinnamate) Benzene-1,3,5-tricarboxamides, *Angew. Chem. Int. Ed.*, **2014**, *53*, 13424-13428
- 86.** M. Konda, S. Bhowmik, S. M. Mobin, S. Biswas, A. K. Das, Modulating Hydrogen Bonded Self-assembled Patterns and Morphological Features by a Change in Side Chain of Third Amino Acid of Synthetic γ -Amino Acid Based Tripeptides, *Chemistry Select*, **2016**, *1*, 2586-2593
- 87.** S. Cantekin, T. F. A. Greef, A. R. A. Palmans, Benzene-1,3,5-tricarboxamide: a versatile ordering moiety for supramolecular chemistry, *Chem. Soc. Rev.*, **2012**, *41*, 6125-6137
- 88.** J. Kong, S. Yu, Fourier Transform Infrared Spectroscopic Analysis of Protein Secondary Structures, *Acta Biochimica et Biophysica Sinica*, **2007**, *39*, 549-559
- 89.** I. Maity, D. B. Rasale, A. K. Das, Peptide nanofibers decorated with Pd nanoparticles to enhance the catalytic activity for C–C coupling reactions in aerobic conditions, *RSC Adv.*, **2014**, *4*, 2984-2988

90. S. M. Kelly, T. J. Jess, N. C. Price, How to study proteins by circular dichroism, *Biochimica et Biophysica Acta*, **2005**, *1751*, 119-139
91. S. Cantekin, D. W. R. Balkenende, M. M. J. Smulders, A. R. A. Palmans, E. W. Meijer, The effect of isotopic substitution on the chirality of a self-assembled helix, *Nature Chemistry*, **2011**, *3*, 42-46
92. A. Desmarcheilier, M. Raynal, P. Brocorens, N. Vanthuyne, L. Bouteiller, Revisiting the assembly of amino ester-based benzene-1,3,5-tricarboxamides: chiral rods in solution, *Chem. Commun.*, **2015**, *51*, 7397-7400
93. S. Cantekin, T. F. A. d. Greel, A. R. A. Palmans, Benzene-1,3,5-tricarboxamide: a versatile ordering moiety for supramolecular chemistry, *Chem. Soc. Rev.*, **2012**, *41*, 6125-6137
94. J. Hu, T. Kurokawa, K. Hiwatashi, T. Nakajima, Z. L. Wu, S. M. Liang, J. P. Gong, Structure Optimization and Mechanical Model for Microgel-Reinforced Hydrogels with High Strength and Toughness, *Macromolecules*, **2012**, *45*, 5218-5228
95. Y. Hu, W. Gao, F. Wu, H. Wu, B. He, J. He, Low molecular weight gels induced differentiation of mesenchymal stem cells, *J. Mater. Chem. B*, **2016**, *4*, 3504-3508
96. S. W. Liao, T. B. Yu, Z. Guan, De Novo Design of Saccharide–Peptide Hydrogels as Synthetic Scaffolds for Tailored Cell Responses, *J. Am. Chem. Soc.*, **2009**, *131*, 17638-17646
97. V. A. Mallia, M. George, D. L. Blair, R. G. Weiss, Robust Organogels from Nitrogen-Containing Derivatives of (*R*)-12-Hydroxystearic Acid as Gelators: Comparisons with Gels from Stearic Acid Derivatives, *Langmuir*, **2009**, *25*, 8615-8625
98. Y. Misawa, N. Koumura, H. Matsumoto, N. Tamaoki, M. Yoshida, Hydrogels Based on Surfactant-Free Ionene Polymers with *N,N'*-(*p*-Phenylene)dibenzamide Linkages, *Macromolecules*, **2008**, *41*, 8841-8846